



ESPE
UNIVERSIDAD DE LAS FUERZAS ARMADAS
INNOVACIÓN PARA LA EXCELENCIA

DEPARTMENT OF ENERGY AND MECHANICS SCIENCES

MECHANICAL ENGINEERING CAREER

**RESEARCH PROJECT, PRIOR TO THE OBTAINING OF THE
MECHANICAL ENGINEER DIPLOMA**

**NUMERICAL ANALYSIS OF A H₂ICE-BASED CHP UNIT FOR USE IN
DECENTRALIZED RENEWABLE ENERGY SYSTEMS**

AUTHOR: BÁEZ MALDONADO, ANDRÉS FERNANDO

PROMOTORS:

PhD: GOYOS PÉREZ, LEONARDO, ESPE

PhD: VERHELST, SEBASTIAN, UGENT

ECUADOR - BELGIUM



2018



CERTIFICADO DEL DIRECTOR



DEPARTAMENTO DE CIENCIAS DE LA ENERGÍA Y MECÁNICA
CARRERA DE INGENIERÍA MECÁNICA

CERTIFICACIÓN

Certifico que el trabajo de titulación, "NUMERICAL ANALYSIS OF A H2ICE-BASED CHP UNIT FOR USE IN DECENTRALIZED RENEWABLE ENERGY SYSTEMS" fue realizado por el señor Báez Maldonado, Andrés Fernando el mismo que ha sido revisado en su totalidad, analizado por la herramienta de verificación de similitud de contenido; por lo tanto cumple con los requisitos teóricos, científicos, técnicos, metodológicos y legales establecidos por la Universidad de Fuerzas Armadas ESPE, razón por la cual me permito acreditar y autorizar para que lo sustente públicamente.

Sangolquí, 6 de agosto de 2018

Firma:



Goyos Pérez, Leonardo

C. C. 1757783525

AUTORÍA DE RESPONSABILIDAD



DEPARTAMENTO DE CIENCIAS DE LA ENERGÍA Y MECÁNICA

CARRERA DE INGENIERÍA MECÁNICA

AUTORÍA DE RESPONSABILIDAD

Yo, Báez Maldonado, Andrés Fernando, declaro que el contenido, ideas y criterios del trabajo de titulación: "NUMERICAL ANALYSIS OF A H₂ICE-BASED CHP UNIT FOR USE IN DECENTRALIZED RENEWABLE ENERGY SYSTEMS" es de mi autoría y responsabilidad, cumpliendo con los requisitos teóricos, científicos, técnicos, metodológicos y legales establecidos por la Universidad de Fuerzas Armadas ESPE, respetando los derechos intelectuales de terceros y referenciando las citas bibliográficas. Consecuentemente el contenido de la investigación mencionada es veraz.

Sangolquí, 17 de agosto de 2018

Firma

Báez Maldonado, Andrés Fernando

C.C.. 060378367-1

AUTORIZACIÓN



DEPARTAMENTO DE CIENCIAS DE LA ENERGÍA Y MECÁNICA

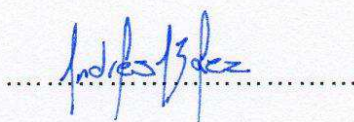
CARRERA DE INGENIERÍA MECÁNICA

AUTORIZACIÓN

Yo, Báez Maldonado, Andrés Fernando autorizo a la Universidad de las Fuerzas Armadas ESPE publicar el trabajo de titulación: "NUMERICAL ANALYSIS OF A H2ICE-BASED CHP UNIT FOR USE IN DECENTRALIZED RENEWABLE ENERGY SYSTEMS" en el Repositorio Institucional, cuyo contenido, ideas y criterios son de mi responsabilidad.

Sangolquí, 17 de agosto de 2018

Firma



Báez Maldonado, Andrés Fernando

C.C.. 060378367-1

DEDICATION

To my heavenly father, for being the one who urged me to try what was seen as a utopia and who never left me alone in the whole journey.

To my parents, for being the breath of a dreamer son, for the gift of the University, the trip, and the life, I love you dad and mom.

To my life advisors, Majo, José, Ale, David, Jos, Tani and Luchito; sharing the path with you is the best gift I have ever had.

To all those who formed, conform and will be part of “ESPE al Máximo”; more than a club, you were my protection, my guide, my beloved ones, and even today, my family. Keep being light, always.

To Wisnner, Roger, Victor, Carlitos, Nelson, John, Andrew, and all who will come; this victory is also yours.

DEDICATORIA

A mi padre celestial, por ser el que me impulso a intentar lo que se veía como una utopía y nunca soltar mi mano en todo el trayecto.

A mis padres, por ser el aliento de un hijo soñador, por el regalo de la universidad, el viaje, y la vida, los amo papitos.

A mis consejeros de vida, Majo, José, Ale, David, Jos, Tani y Luchito; compartir el camino con ustedes es el mejor regalo que he tenido.

A todos los que conformaron, conforman y conformarán ESPE al Máximo, porque más que un club, fueron mi protección, mi guía, mis amados, y aún hoy, mi familia. Sigán siendo luz, siempre.

A Wisnner, Roger, Víctor, Carlitos, Nelson, Jhon, Andrew, y todos los que vendrán; esta victoria también es suya.

ACKNOWLEDGMENTS

To Roger & Emilia, for making me feel at home.

To Leonardo, Roger, Sebastian & Louis, for being my mentors.

To Duc-Khanh, Stijn, Gilles, Jeroen, Haohan, Ahmed & Roel; for making me feel part of the research group.

To Van Wingen nv, for giving me the opportunity of being part of this big project.

To Bavo, for being a great partner on this project; we did a great team.

To Koen, Griet & Annie, for making a great work always.

To Eddy, Cris & all the church "Unidos en Cristo", for being my family on Belgium.

AGRADECIMIENTO

A Roger y Emilia, por hacerme sentir en casa.

A Leonardo y Sebastian, por ser mis mentores.

A Duc-Khanh, Stijn, Gilles, Jeroen, Haohan, Ahmed y Roel; por hacerme sentir parte del grupo de investigación.

A Van Wingen nv, por darme la oportunidad de formar parte de este gran proyecto.

A Bavo, por ser una gran ayuda en las pruebas del motor; hicimos un gran equipo.

A Koen, Griet y Annie, por hacer un gran trabajo siempre.

A Eddy, Cris y toda la iglesia “Unidos en Cristo”, por ser mi familia en Bélgica.

CONTENTS

CERTIFICADO DEL DIRECTOR.....	i
AUTORÍA DE RESPONSABILIDAD.....	ii
AUTORIZACIÓN	iii
DEDICATION	iv
DEDICATORIA.....	v
ACKNOWLEDGMENTS	vi
AGRADECIMIENTO.....	vii
CONTENTS.....	viii
TABLES.....	xii
FIGURES.....	xiii
NOMENCLATURE	xiv
RESUMEN.....	xviii
ABSTRACT	xix
CHAPTER I	1
1. Background and goal statement.....	1
1.1. The project.....	1
1.2. Justification	2
1.2.1. Technical & Environmental Justification.....	2
1.2.2. Legal justification	3
1.2.3. Academic Justification	4

1.3. Goal statement.....	4
1.4. Research goals	5
CHAPTER II	6
2. Literature review.....	6
2.1. Decentralized energy systems	6
2.2. Cogeneration.....	9
2.2.1. Optimum CHP selection.....	13
2.2.2. Electric priority and thermal priority.....	14
2.2.3. Emissions standards for CHP-units	15
2.3. Hydrogen as fuel	16
2.3.1. Hydrogen properties	17
2.3.2. Abnormal combustion	18
2.4. Hydrogen-Fueled internal combustion engines.....	19
2.4.1. Conversion of an engine to hydrogen operation	19
2.4.2. Air-fuel ratio	22
2.4.3. NOx formation.....	26
2.4.4. Engine parameters influence over performance	27
CHAPTER III	34
3. Thermic design.....	34
3.1. Definition of the engine operating conditions	34
3.2. Baseline of the project.....	36

3.2.1. Global heat balance	39
3.2.2. Coolant properties.....	40
3.2.3. Fuel power	40
3.2.4. Thermal power available for recovery	40
3.2.5. Thermal power available on the exhaust gases	41
3.2.6. Hydrogen combustion – chemical equation	42
3.2.7. Properties of the exhaust gases.....	42
CHAPTER VI.....	45
4. Experimental tests of engine-settings influence over power and emissions	45
4.1. Experimental design.....	45
4.2. Effect of engine factors over power distribution.....	46
4.2.1. Start of Injection	46
4.2.2. Ignition Timing.....	51
4.2.3. Injection Pressure	58
4.3. part load and higher power	61
4.3.1. Thermal power available at part load	62
4.3.2. Higher electric power test	65
4.4. Optimized maps	67
4.5. Power-to-heat ratio and primary energy savings	69
4.5.1. Power-to-heat ratio estimation (<i>C_{design}</i>)	69
4.5.2. Primary Energy Saving Ratio	70

CHAPTER V	71
5. Conclusions.....	71
5.1. Conclusions and optimized settings	71
5.1.1. Start of Injection	71
5.1.2. Spark timing	72
5.1.3. Injection Pressure	72
5.1.4. Two ignition maps?	73
5.1.5. Power-to-heat ratio and primary energy savings	74
5.2. Recommendations for future work	75
5.2.1. General recommendations.....	75
5.2.2. Recommendations for the conversion of the 4.2 liters engine	76
REFERENCES	77

TABLES

Table 1 <i>Engine data</i>	2
Table 2 <i>Power generation technologies.</i>	8
Table 3 <i>Hydrogen properties</i>	17
Table 4 <i>Influence of the richness of the mixture over performance in PFI-H₂-ICEs</i>	23
Table 5 <i>Influence of the richness of the mixture over performance (continue)</i>	24
Table 6 <i>Work settings</i>	35
Table 7 <i>Sensors and measurement equipment</i>	36
Table 8 <i>Enthalpy of formation of common combustion species</i>	44
Table 9 <i>Latent heat of common products of hydrogen combustion</i>	44
Table 10 <i>Experimental investigation planning</i>	45
Table 11 <i>Spark Timing zones characteristics</i>	53
Table 12 <i>Baseline from the previous phase</i>	61

FIGURES

<i>Figure 1.</i> Equivalence ratio distribution under different SOI.....	31
<i>Figure 2.</i> Layout of the CHP unit configuration.	38
<i>Figure 3.</i> Heat Balance on the generating group.	39
<i>Figure 4.</i> Start of Injection test settings.	47
<i>Figure 5.</i> Electric Power & Exhaust Gases Temperature vs. Start of Injection.	48
<i>Figure 6.</i> NO emissions vs. start of injection.....	50
<i>Figure 7.</i> Performance curve at 9kW for various spark timing.	54
<i>Figure 8.</i> Efficiency of electrical power production.....	55
<i>Figure 9.</i> Influence of ST on power distribution at 9kWe.	57
<i>Figure 10.</i> Injection pressure influence over exhaust temperature.	59
<i>Figure 11.</i> Injection pressure influence over NO emissions.....	60
<i>Figure 12.</i> Total Heat Available by retarding the ST. (IP=1.5 bar)	63
<i>Figure 13.</i> Fuel consumption vs spark timing. (IP=1.5 bar)	64
<i>Figure 14.</i> Electric Efficiency at part loads and higher loads. (IP=1.5 bar)	65
<i>Figure 15.</i> Emissions at higher loads. (IP=1.5 bar).....	66
<i>Figure 16.</i> MBT and Minimum Retard to reduce NOx. (IP=1.5 bar).....	67
<i>Figure 17.</i> Electric efficiency of both mappings. (IP=1.5 bar)	68
<i>Figure 18.</i> Power to heat ratio.	70
<i>Figure 19.</i> Primary Energy Saves Ratio.	70

NOMENCLATURE

Symbols

\dot{m}	mass flow
F	Fuel power
\dot{E}	Electrical Power
\dot{Q}	Thermal Power
\dot{H}	Thermal Power Available
UTS	Exhaust Gases Temperature
TS	Fluid Temperature
\bar{T}	Average temperature
cp	Specific heat at constant pressure
η	Efficiency
λ	Air/Fuel Equivalence Ratio
ϕ	Fuel/Air Equivalence Ratio
ρ	Density
N	Number of moles
M	Molar mass
h	enthalpy
y	molar fraction

Subscripts

<i>f</i>	Fuel
<i>exh</i>	Exhaust Gases
<i>cool</i>	Coolant
<i>HEX</i>	Heat Exchanger
<i>abs</i>	absorbed
<i>gen</i>	generator
<i>in</i>	intake
<i>a</i>	air
1	Primary circuit
2	Secondary circuit
<i>et</i>	Ethylene glycol
<i>p</i>	Pump
<i>hsys</i>	Heat system (control volume)
<i>disp</i>	Dissipated
<i>s</i>	stoichiometric

Abbreviations

aTDC	after top dead center
BMEP	Brake Mean Effective Pressure
BRoPT	Best Result of Previous Test

bTDC	before top dead center
°CA	crank angle degrees
CFR	Cooperative Fuel Research
CHP	cogeneration of heat and power
CNG	Compressed Natural Gas
CR	compression ratio
DI	direct injection
DISI	direct injection spark ignited
EGR	exhaust gas recirculation
EVC	exhaust valve closing time
EVO	exhaust valve opening time
FC	fuel cell
H ₂	hydrogen
ICE	internal combustion engine
IVC	inlet valve closing time
IVO	inlet valve opening time
LHV	Lower Heat Value
MAP	manifold air pressure
MBT	minimum spark advance for best torque (°CA BTDC)
MPbEL	Maximum Power below Emissions
Nm ³	Normal cubic meters or cubic meters at normal conditions, see NTP
NO	Nitrogen monoxide
NO ₂	Nitrogen dioxide

NO _x	Nitrogen oxides
NTP	normal temperature and pressure (300 K and 1 atm)
PFI	port fuel injection
rpm	revolutions per minute
SAE	Society of Automotive Engineers
SI	spark ignition
SOI	start of injection
ST	spark timing
SULEV	Super Ultra Low Emission Vehicle
TDC	top dead center
TLEV	Transitional Low Emission Vehicle
WOT	wide open throttle

RESUMEN

La lucha para disminuir las emisiones de efecto invernadero ha sido un tema de discusión durante décadas. Hoy en día, las compañías de generación de energía tienen la presión de buscar formas más eficientes de producir energía y al mismo tiempo reducir las emisiones. Una solución a esto son los sistemas de energía descentralizados con aprovechamiento de calor o CHP, los cuales no solo tienen la facilidad de generar electricidad in situ y evitar así pérdidas de energía por distribución y conversión de alta a baja tensión, sino que también tienen la posibilidad de convertir gran parte de las pérdidas de calor en calor útil. La empresa patrocinadora, Van Wingen nv, que ha estado involucrada en el negocio de los generadores eléctricos desde 1970, adicionalmente a los beneficios de una unidad CHP busca ofrecer soluciones con emisiones casi nulas. Como resultado, el proyecto redactado en este documento se centra en la optimización de un motor a hidrógeno de encendido por chispa de 1.8 litros para obtener 9kWe con emisiones de NOx minimizadas. También se reporta una estimación de la relación electricidad-calor y del ahorro de energía primaria para garantizar una cogeneración de alta eficiencia. Finalmente, dos mapas de ignición optimizados, uno para mayor potencia y otro para mínimas emisiones, se reportan en este documento.

PALABRAS CLAVE:

- **MOTOR A HIDRÓGENO**
- **UNIDAD DE COGENERACIÓN**
- **RELACIÓN ENTRE ELECTRICIDAD Y CALOR**
- **ENERGÍA DESCENTRALIZADA**

ABSTRACT

The fight to diminish greenhouse emissions has been a topic of discussion for decades. Nowadays, energy generation companies have the pressure of looking for more efficient ways to produce energy while lowering the emissions. As solution, ICE-based decentralized energy systems have the advantage to provide electricity in-situ, avoiding the power losses due to distribution lines and conversion from high to low voltage, as well as having the possibility of convert great part of the heat losses into useful heat. Furthermore, Van Wingen nv, the sponsor enterprise which has been involved on the business of electric generators since 1970, is looking forward to provide near zero emissions solutions. As result, the project reported in this document mainly focuses on the optimization of a 1.8-liter spark-ignited hydrogen-engine provided by the enterprise in order to get 9kWe with near zero NOx emissions. In addition, an estimation of the power-to-heat ratio and primary energy savings was done to ensure the system will provide a high-efficiency cogeneration. Finally, two optimized ignition maps, one for the highest power and one optimized to get lower emissions, are documented on this paper.

KEYWORDS:

- **HYDROGEN ENGINE**
- **CHP UNIT**
- **POWER-TO-HEAT RATIO**
- **DECENTRALIZED ENERGY**

CHAPTER I

BACKGROUND AND GOAL STATEMENT

1.1. THE PROJECT

On 2014, the company E. Van Wingen nv, which has been involved on the business of electric generators since 1970, started a decentralized energy generation project based on hydrogen engines in collaboration with Ghent and VIVES Universities. The project had been divided into two phases: the first phase of the project was the conversion of a 1.8-liter spark-ignited engine (Table 1) to work with hydrogen as fuel; from this first phase, the result was a maximum power output of 9kWe at an air-fuel equivalence ratio of two ($\lambda = 2$) with 28% electrical efficiency. The second phase¹, redacted on this document, is the optimization of the mentioned engine in order to get the lowest NOx emissions possible at the maximum power output encountered on the first phase, 9kWe, without compromising the global efficiency of the system, and also the study of the influence of engine settings over the power-to-heat ratio and how this affects the performance of the CHP-unit. The results of the project will be used in the future as basepoint for the conversion and optimization of a 4.2 liter engine to hydrogen as part of an environmentally friendly CHP-unit.

¹ The second phase, not as the first one, takes on account the heat that can be used by the CHP-unit.

Table 1*Engine data*

Parameters	
Manufacturer	Lister Petter
Model	LPWG-4
Origin	United Kingdom
# cylinders and alignment	4 in line
Compression ratio	9.5:1
Piston diameter	86 mm
Stroke	80 mm
Swept volume	1.86 liters
Starting order	1-3-4-2
Air intake	Naturally aspirated

1.2. JUSTIFICATION

1.2.1. Technical & Environmental Justification

Decentralized energy systems allow to provide energy to rural or isolated areas, as well as to urban areas, being not only a solid solution for harsh places but also a preventive solution to the potential saturation of the electric distribution networks due to the exponential growth of the population. In addition to this, when using hydrogen as fuel, CO₂ emissions are zero², which contributes to the conservation of the environment, and

² CO₂ emissions are produced only by the burning of the oil that sweeps through the piston rings into the combustion chamber. In any case, CO₂ emissions due to what was mentioned are negligible.

also proposes an alternative energy supply to natural reserves. Moreover, to analyze the possibility of varying the power-to-heat ratio of an ICE-based CHP can lead to achieve a better coupling to the user's energy demand in the future, thus producing greater primary energy saving and therefore a shorter payback period. Regarding the variation of the power-to-heat ratio produced by a CHP-unit, there isn't information available about any research on the topic.

1.2.2. Legal justification

The project is in line with objectives 3, 7 and 11 of the Ecuadorian National Plan for Good Living (Plan Nacional del Buen Vivir), which are:

- Objective 3. Improve the quality of life of the population.
- Objective 7. Guarantee the rights of nature and promote territorial and global environmental sustainability.
- Objective 11. Ensure the sovereignty and efficiency of the strategic sectors for industrial and technological transformation.

Additionally, this project is aligned with the objectives of the Paris agreement, and with the proposal of Ecuador with respect to it, to reduce emissions from the energy sector,

which currently represent 50% of the country's emissions, in 20.4 % -25% for the year 2025.^{3,4}

1.2.3. Academic Justification

The project benefits to University of the Armed Forces – ESPE by being an international-interest research topic carried out in collaboration with UGent, a top-100 world ranking university, enhancing its prestige as an A-class university and contributing to the fulfillment of the accreditation requirements of the Mechanical Engineering Career.

1.3. GOAL STATEMENT

From the literature its known:

- The efficiency of a hydrogen engine is highly dependent on ignition timing as function of fuel richness (Sierens & Verhelst, 2000; Subramanian, Mallikarjuna, & Ramesh, 2007). That means thermal efficiency is also changing and therefore the power-to-heat ratio may be variated by changing the ignition timing.

³ Font: (WWF, n.d.)

⁴ The commitment to the proposal of the Paris Agreement was ratified with the signature of President Lenin Moreno on July 29, 2017. (Diario El Universo, 2017)

- The optimal selection of a micro-CHP unit corresponds to the smallest gap between the primary-mover's maximum power output and the maximum power demand of the facility, as well as a power-to-heat ratio of the CHP that better fits the demanded annual power-to-heat ratio of the customer. (Barbieri, Spina, & Venturini, 2012). That means that a variable power-to-heat ratio may offer great primary energy savings and therefore money savings for the CHP-unit customer.

According to that, and beside the optimization of the engine to get near zero emissions at full load (9kWe), this project looks to answer the following question:

¿How much does the power-to-heat ratio of a hydrogen internal combustion engine can be varied without modifying its physical settings, and how does this affect to the performance of the engine in dependence of a determined demand?

1.4. RESEARCH GOALS

1. Optimize the engine settings in order to get the lowest emissions possible at 9kWe without compromising the global efficiency of the CHP-unit.
2. Quantify how much the power-to-heat ratio of the CHP-unit varies when the engine settings are changed, and its influence over the engine performance.
3. Calculate the primary energy savings of the CHP unit using 120°C as design temperature of the exhaust gases in order to guaranty a high-efficiency operation for all the variation range of power-to-heat ratio.

CHAPTER II

LITERATURE REVIEW

2.1. DECENTRALIZED ENERGY SYSTEMS

Centralized electricity generation is the most common way to generate electricity and it's done in large power plants to meet the demand of entire cities. The energy produced in these plants must then be transmitted dozens or even hundreds of kilometers before reaching the user, for which the power losses in the distribution network oscillate between 7 and 10%. In addition, the facilities associated with the distribution network account for 30% of the investment in a centralized generation project. (Romero, 2014)

Due to this, and to the expansion of cities due to population growth, decentralized production has been proposed as a solution within the concept of smart cities. Decentralized or distributed energy production, according to the Commission of Regional Energy Integration⁵ (CIER), are small units (<5MWe) connected to the low-voltage network and located at the point of consumption (Durán, 2012). Other international institutions⁶ also include medium-scale generation (<50MWe) connected to voltage levels of 110 kV or lower (Scheepers, et al., 2007; FENERCOM, 2007; OJ L 211, 14.8.2009, p. 55–93; Policy Department A: Economic and Scientific Policy, 2010; Durán, 2012).

⁵ Non-Governmental Organization of the electricity sector of the Ibero-American countries.

⁶ DOE (US) & Special Regime (Spain).

Romero (2014) establishes that there are several reasons why the development of distributed production should be promoted:

1. Relief of the saturation of the transport and distribution system.
2. Reduction of losses in the network and associated costs.
3. Greater ease and lower installation, operation and maintenance costs.
4. Reduction of the use of common energy to avoid its depletion.⁷
5. Reduction of polluting emissions according to the Paris Agreement.⁸
6. Improvement of the continuity of the electric service.
7. Promotion of private investment.
8. Coverage of isolated regions.

Table 2 shows a comparison of the available decentralized generation technologies in the world market. These technologies can be classified according to their maturity in mature, semi-mature and emerging. The mature ones are alternative engines, gas turbines, mini hydraulic, winds, solar-thermal, photovoltaic. The semi-mature technologies are biomass, microturbines and fuel cells. Marine and geothermal are considered emerging technologies, for which they were not included in the mentioned table.

⁷ Depletion time according to Romero (2014): carbon: 200-250 years, uranium 70-90 years, natural gas 60-80 years, petroleum 40-50 years.

⁸ Agreement signed on 2015, successor of the Kyoto protocol of 1997, with the goal of reducing de greenhouse emissions.

Table 2*Power generation technologies.*

TECHNOLOGY	PRIMARY ENERGY	POWER	EFFICIENCY (%)	INVESTMENT (€/kW)
Alternative engines	CNG, diesel, biogas, propane	5kW-20MW	28-42% (CNG) 30-50% (diesel) 80-90% (CHP)	500-900
Gas turbines	CNG, biogas, propane	250kW-500MW	25-60% 70-90% (CHP)	>600 1400 (CHP)
Mini hydraulic	Water	10kW-10MW	80-90%	1000-1800
Wind energy	Wind	5kW-5MW	43%	1100-1700
Solar-thermal	Sun	0,2kW-200MW	13-21%	3500-8000
Photovoltaic	Sun	<1kW-0.1MW	14%	5000-7000
Biomass	Biomass		32%	1500-2500
Microturbines	CNG, H2, biogas, propane, diesel,	25kW-0,4MW	25-30% 85% (CHP)	900- 2000
Fuel cells	CNG, H2, methane, propane.	1kW-11MW	35-65% 90% ^a (CHP)	2500-3700

CNG: Compressed Natural Gas. H2: hydrogen. CHP: Cogeneration of heat and power. Data from 2004 (conversion 1€=1.3666 \$)

Font: Durán (2012) p.57. ^a (E. Van Wingen nv, 2017)

2.2. COGENERATION

Bearing in mind that the conversion of chemical energy into electricity in exothermic process releases a large amount of heat, internal combustion engines are classified as inefficient machines, because the energy losses in this conversion reach over 50% of the caloric power of the fuel. However, the efficiency of these machines can be improved by taking advantage of the heat released to provide hot air or water, achieving an overall efficiency of up to 90%⁹. The machines that are able to generate electricity as well as taking advantage of the residual heat for the benefit of the user are called CHP units.

According to the European Union, cogeneration is defined as "the simultaneous generation of thermal energy and electrical or mechanical energy in a single process", therefore, a cogeneration unit is one in which the process performed meets the definition mentioned above. Table 2 shows several technologies usually used for cogeneration (specified in parentheses as "CHP") and the increase in efficiency obtained when using a primary mover for cogeneration purposes.

For a better understanding of the advantages of a CHP unit it's necessary to review the terms used by European Union in its Official Journal; according to it the following definitions are established.

'useful heat' shall mean heat produced in a cogeneration process to satisfy an economically justifiable demand for heat or cooling;

⁹ Efficiency of an ICE-based mini-CHP-unit from E. Van Wingen nv. Font: E. Van Wingen nv (2017)

'electricity from cogeneration' shall mean electricity generated in a process linked to the production of useful heat and calculated in accordance with the methodology laid down in Annex I;

'overall efficiency' shall mean the annual sum of electricity and mechanical energy production and useful heat output divided by the fuel input used for heat produced in a cogeneration process and gross electricity and mechanical energy production;

'power to heat ratio' shall mean the ratio between electricity from cogeneration and useful heat when operating in full cogeneration mode using operational data of the specific unit;

'micro-cogeneration unit' shall mean a cogeneration unit with a maximum capacity below 50 kWe;

'small scale cogeneration' shall mean cogeneration units with an installed capacity below 1 MWe; (OJ L 315, 14.11.2012, p. 1–56)

The European Union has also provided a document that establishes certain guidelines determining the numerical values of the definitions cited above¹⁰. However, these guidelines are only in words, hindering the efficient application of them, says Frangopoulos (2012), who, in his publication, breaks down a complete procedure that facilitates the understanding of what has been established by the European Commission.

¹⁰ Commission Decision of 19 November 2008, Current document (OJ L 338, 17.12.2008, p. 55-61, 17.12.2008).

Based on the two mentioned publications, the terminology and equations used in this project were established:

E Electricity produced in a reference period at specific load^{11,12}.

H_{CHP} Useful heat produced for the CHP in the same period as E .

F Fuel energy, in means of the lower heating value, used for the CHP to produce E y H_{CHP} .

η_e Efficiency of the CHP-unit for producing E . From now on called “electric efficiency”.

$$\eta_e = \frac{E}{F} \quad (2.1)$$

η_h Efficiency of the CHP-unit for producing H_{CHP} . From now on called “thermal efficiency”.

$$\eta_h = \frac{H_{CHP}}{F} \quad (2.2)$$

η Global efficiency of the CHP-unit.

$$\eta = \eta_e + \eta_h \quad (2.3)$$

C Power to heat ratio of the CHP-unit on full cogeneration mode.¹³

$$C = \frac{E}{H_{CHP}} = \frac{\eta_e}{\eta_h} = \frac{\eta_e}{\eta - \eta_e} \quad (2.4)$$

¹¹ For calculation purposes, the Commission Decision assumes a value of 1 for the conversion form mechanical energy into electricity. (OJ L 338, 17.12.2008, p. 55-61)

¹² The Commission Decision stablishes a minimum reference period of one hour and maximum of one year. (OJ L 338, 17.12.2008, p. 55-61)

¹³ C corresponds to the power-to-heat ratio design, mentioned on numeral 7.4. of the Commission Decision’s Annex, of 19 of november of 2008. (OJ L 338, 17.12.2008, p. 55-61)

η_{er} & η_{hr} Reference values of the efficiency of producing power and heat separately respectively. $\eta_{er} = 44.2\%$ & $\eta_{hr} = 90\%$ from the Official Journal of the European Union.¹⁴

F_{er} Fuel energy needed for the separated generation of E on the reference system.

$$F_{er} = \frac{E}{\eta_{er}} \quad (2.5)$$

F_{hr} Fuel energy needed for the separated generation of H_{CHP} on the reference system.

$$F_{hr} = \frac{H_{CHP}}{\eta_{hr}} \quad (2.6)$$

PES Primary energy savings

$$PES = (F_{er} + F_{hr}) - F \quad (2.7)$$

$PESR$ Primary energy savings ratio.¹⁵

$$PESR = \frac{PES}{F_{er} + F_{hr}} = 1 - \frac{1}{\frac{\eta_e}{\eta_{er}} + \frac{\eta_h}{\eta_{hr}}} \quad (2.8)$$

From equations (2.1) – (2.4) the primary energy savings ratio can be obtained as function of the power-to-heat ratio.¹⁶

$$PESR = 1 - \frac{1 + C}{\eta \left(\frac{C}{\eta_{er}} + \frac{1}{\eta_{hr}} \right)} \quad (2.9)$$

¹⁴ Available on the annex II of the Commission Delegated Regulation (EU) 2015/2402, of 12 October 2015. (OJ L 333, 19.12.2015, p. 54–61)

¹⁵ This ratio has to be at least 0.1 for cogeneration and greater than zero for small scale or micro cogeneration to be considered as high efficiency cogeneration. (OJ L 315, 14.11.2012, p. 1–56)

¹⁶ This equation was used some years before the European Commission documents mentioned before were available. (CRES & ZREU, 2001)

The numeral 7.4. of the Annex to the Commission Decision, of 19 November 2008, establishes that for cogeneration units under development, the design power-to-heat ratio in full cogeneration mode (equation (2.4)) can be used. According to the mentioned document:

A cogeneration unit operating with maximum technically possible heat recovery from the cogeneration unit itself is said to be operating in full cogeneration mode. The heat has to be produced at the site pressure and temperature levels required for the specific useful heat demand or market. In the case of full cogeneration mode, all electricity is considered combined heat and power (CHP) electricity. (OJ L 338, 17.12.2008, p. 55-61)

In this way, the equations establish above are according the European Commission requirements.

2.2.1. Optimum CHP selection

According to Barbieri, Spina, & Venturini (2012), the optimum selection of a micro-CHP unit for residential applications depends on two main factors: electricity production, and power-to-heat ratio. According to the payback period and Net Present Value (VAN)¹⁷, the optimal selection of a micro-CHP corresponded to the lower gap between the electric

¹⁷ Calculated for 15 years.

output of the CHP and the maximum electrical demand $((P_e)_{PM} - (P_e)_{dem_max})$, and a power-to-heat ratio of the CHP that fits better with the annual demanded power-to-heat ratio of the consumer.

2.2.2. Electric priority and thermal priority

In the research carried out by Caresana, Brandoni, Feliciotti, & Bartolini (2011), two priority modes are proposed for the control of the CHP-unit: electric priority and thermal priority. In the specific case of the authors, the generation is carried out with a variable speed asynchronous generator with an anti-wind-up and saturation PI controller to prevent the demand of negative torques or greater than the instantaneous speed. In this way, in electrical priority, the regulator is based on an optimization table that, for a given power, selects the speed related to the highest electrical efficiency. On the other hand, in thermal priority, the controller calculates the electrical power according to the water temperature required at the output of the cogeneration unit.

For the evaluation of the two control modes the demand of the average day of January and July was taken as representation of winter and summer seasons respectively, for which three cases were studied: a building of 10 apartments, an office and a hotel. The results of this research showed that the advantages of a variable speed asynchronous engine-generator coupling compared to a constant speed synchronous one is relevant only at low loads. Regarding the type of control, the thermal priority mode showed benefits

reflected in daily monetary savings (euros/day) only for the case of the building of 10 apartments in winter season, working with an asynchronous motor (10% improvement).

2.2.3. Emissions standards for CHP-units

For the Flemish region, in the article 5.43.2.2 of the VLAREM II environmental regulations law (VLAREM II, article 5.43.2, 2018-05-04), it is mentioned that for internal combustion engines that use gaseous fuel with a nominal thermal input of less than 300kW, no emission limits are applied. For engines with a nominal thermal input greater than 300kW and less than 5MW, the maximum allowed limit of NO_x emissions is 95mg / Nm³¹⁸, on exception of using other fuel than natural gas or dual fuels in gas mode; for this exception a limit value of 190 mg/Nm³ is established. The percentage of correction oxygen for stationary engines is set as 15%.¹⁹

For VLAREM II, NO_x emissions have to be reported as mg/Nm³ in NO₂ mass basis. That means that the molecular weight of the NO₂ (46g/mol), which is higher than for NO (30g/mol), is selected to establish the worst-case scenario (Global Combustion Systems, w.d.; Sira Certification Service, 2014). In that way, NO_x emissions were established as:

$$Concentration[ppm] \times \frac{molecular\ weight}{molar\ volume} = Concentration \left[\frac{mg}{m^3} \right] \quad (2.10)$$

$$NO_x[ppm] \times \frac{46}{22.4} = NO_x \frac{mg}{Nm^3} \quad (2.11)$$

¹⁸ Regulations valid until December 31, 2024. VLAREM II, Article 5.43.2.15 y 16.

¹⁹ VLAREM II, Article 5.43.2.2, 2nd paragraph.

Also, to apply the regulations requirements, measurements must be corrected at 15% oxygen content with the formula bellow:

$$E_c = \frac{21 - O_c}{21 - O_m} \cdot E_m \quad (2.12)$$

Where:

E_c : corrected emission concentration (mg/Nm³) in dry base

E_m : measured emission concentration (mg/Nm³) in dry base

O_c : Correcting oxygen (O₂) percentage (%) (15% for stationary engines)

O_m : measured oxygen (O₂) percentage (%) (Annex 3 of Book VI of the unified text from the secondary legislation of the Environmental Ministry, 2015)

2.3. HYDROGEN AS FUEL

In recent decades, concern for pollution and mankind role on it has been notorious, leading the so-called "environmental awareness" to play a decisive function on project planning and daily life. However, to have a significant change, joint and unified participation is necessary, and only achievable through laws. Because of this, it is crucial that executive and legislative bodies lead the control and regulation of greenhouse gas emissions.

Among its objectives of contributing to environmental sustainability, the European Union Member States have committed themselves to reduce greenhouse gas emissions by 80% by 2050 compared to the 1990 emissions, motivating to the research of new

transport technologies and optimized electric generation as well. (European Commission, 2011)

2.3.1. Hydrogen properties

Table 3
Hydrogen properties

Property	Hydrogen	Methane	Iso-octane
Molecular weight (g/mol)	2.016	16.043	114.236
Density (kg/m ³)	0.08891 ^a	0.65	692
Mass diffusivity in air (cm ² /s)	0.61	0.16	~0.07
Minimum ignition energy (mJ)	0.02	0.28	0.28
Minimum quenching distance (mm)	0.64	2.03	3.5
Flammability limits in air (vol%)	4–75	5–15	1.1–6
Flammability limits (λ)	10–0.14	2–0.6	1.51–0.26
Flammability limits (φ)	0.1–7.1	0.5–1.67	0.66–3.85
Lower heating value (MJ/kg)	120	50	44.3
Higher heating value (MJ/kg)	142	55.5	47.8
Stoichiometric air-to-fuel ratio (kg/kg)	34.2	17.1	15
Stoichiometric air-to-fuel ratio (kmol/kmol)	2.387	9.547	59.666

Note: Methane and iso-octane were taken on behalf of natural gas and gasoline respectively. Font: (Verhelst & Wallner, 2009). ^a Taken from appendix 1 of the flow-meter's manual (Bronkhorst, 2008).

The main advantage of having hydrogen as fuel, compared to traditional fuels, rely on the fact that resulting product of theoretically complete combustion is only water vapor. Furthermore, its flammability wide-range allows to work with very lean mixtures as well as stoichiometric. On the other hand, as the lowest-density chemical element, efficient storage for some applications are still case of research. (Verhelst, et al., 2012)

2.3.2. Abnormal combustion

Abnormal combustion is the name for the combustion event that takes place in a different time than ignition and may seriously damage the engine as well as the intake manifold. Regarding hydrogen, and due to its low flammability limit, low density, minimum ignition energy ten times lower than gasoline, and minimum quenching distance three times lower than methane (see Table 3), some safety measures have to be taken to avoid this kind of combustion.

Verhelst et al. (2012) mention three types of abnormal combustion associated with hydrogen: pre-ignition, backfire and autoignition. The pre-ignition is the premature combustion of the fresh mixture in the compression stroke that occurs with the intake valves closed, while the backfire is basically the same phenomenon, but with the intake valves open. As for autoignition, it is the spontaneous combustion of the air-fuel mixture; in other words, the combustion of the mixture without heat source.

Pre-ignition and backfire can be caused by high temperature spots in the walls of the combustion chamber, valves, oil residues, spark plugs, piston head, or residual gases of the previous combustion cycle. Also, these anomalies are more likely to occur when operating the engine at high load and speed, due to the increased temperature on the aforementioned parts, as well as using mixtures close to stoichiometric; this latter is due to hydrogen's minimum ignition energy decrease for lambda values near to one. In addition, the abrupt heating in the combustion chamber because of the pre-ignition produces the ideal environment for backfire to happen in a consecutive cycle. (Verhelst & Wallner, 2009)

Measures to avoid backfire include limiting the end of the injection, leaving no residual mixture in the intake manifold; using direct injection; or optimizing injection with Variable Valve Timing (VVT) for both intake and exhaust. The pre-ignition can be successfully avoided by correct selection criteria²⁰ of the spark plugs, crankcase ventilation, optimized cooling passages near the valves and hot spots, and the use of sodium-filled exhaust valves. Regarding autoignition, it is convenient to work with lean mixtures or low compression ratios to avoid this phenomenon. (Verhelst & Wallner, 2009)

Verhelst & Wallner (2009) argue that working lean has been the choice of many researchers since it successfully avoids abnormal combustion. The authors state that this is due to excess air providing a cooling effect, thus lowering the temperature of all the elements involved on the combustion process. Additionally, this measure increases thermal efficiency and produces non or near zero NOx emissions, although a power-decrease price needs to be paid, the article says.

2.4. HYDROGEN-FUELED INTERNAL COMBUSTION ENGINES

2.4.1. Conversion of an engine to hydrogen operation

In 2009, Verhelst & Wallner devoted an entire chapter to gather the measures taken by different authors for hydrogen-fueled engines design or conversion, ensuring that the

²⁰ For further information refer to (Verhelst & Wallner, 2009)

motivation of most of the measures taken is to avoid abnormal combustion. Both, the main problems that must be considered in the conversion of a spark ignition engine for its proper operation with hydrogen and the solutions cited by the authors mentioned above, are pointed below.

In order to eliminate "hot spots", the authors cited by Verhelst & Wallner (2009) used cold spark plugs; refrigerated exhaust valves; multiple valves per cylinder in order to reduce the thermal load per valve; ashless oil; proper oil control to avoid possible leaks; optimized engine cooling passages; DI or injection delay on PFI to have a pre-cooling of the combustion chamber utilizing the intake air; and optimal evacuation of the combustion gas, for which VVT can be used.

Another factor to prevent abnormal combustion in hydrogen-fueled engines is to control the residual energy of the ignition system, due to the ease of hydrogen combustion even with very low energy loads (See Table 3). For this, Verhelst & Wallner (2009) cite two solutions: grounding the ignition system and avoid to use adjacent cable ignition; coil-on-plug systems fulfill both requirements. Verhelst & Wallner also mention that, unlike what one might believe, hydrogen requires a high-voltage ignition system²¹, which can also be solved using a coil-on-plug system or by reducing the spark plug gap even as small as 0.5mm, which reduces the necessary ignition voltage.

The regulation of the injection is also an important factor in hydrogen engines. It isn't only recommended the delay of the injection to get an air-only cooling effect in the

²¹ Verhelst & Wallner mention that this requirement can be caused by the lower ionic concentration of the hydrogen flame compared to hydrocarbon flame.

combustion chamber, as mentioned above, but also limiting the end of the injection before closing the intake valves to avoid the existence of hydrogen in the intake manifold and the possible backfire that it may cause. The narrowness of resulting injection time generates the need of increased injection flow, which can be solved with multiple injectors (MPI) in the case of indirect injection (PFI), or by using in-cylinder injectors (DI) with flow rates of 4-6g/s at a pressure of 100 Bars. (Verhelst & Wallner, 2009)

To avoid autoignition in a spark-ignited hydrogen engine, as in gasoline engines, the compression ratio must be limited, Verhelst & Wallner (2009) point out. On the other hand, to achieve a compression ratio that provides the highest indicated power as well as an adequate thermal efficiency is desired. In the different investigations cited by the authors, values between 7.5 and 14.5 are used.

Hydrogen also has, among its particularities, extremely high flame speed²² and a minimum extinction distance five times narrower than gasoline. Several investigations cited in Verhelst & Wallner (2009) recommend the use of low turbulence combustion chambers, such as disk or pancake type, to avoid stimulate the flame speed, while decreasing the crevice volumes avoids the possibility of having abnormal combustion due to hot spots in the ring of fire and the minimum quenching distance of hydrogen.

Other measures cited by Verhelst & Wallner (2009) are: use non-platinum spark plugs, since platinum function as an oxidant factor for hydrogen; meticulous selection of compression rings to avoid unburned mixture filtrations to the crankcase; selection of

²² Flame propagation velocity of the flame in hydrogen and gasoline [cm/s]: 290 and 45 respectively at T = 360K, P = 1atm and $\lambda = 1$. Source: Table 2, Verhelst & Wallner (2009).

absence-of-lubrication resistant materials for the design of injectors and valve seats; use of increased-water-concentrations resistant lubricant; and positive ventilation of the crankcase.

2.4.2. Air-fuel ratio

Verhelst (2014) mentions two basic choices of the air-fuel equivalence ratio: stoichiometric ($\lambda = 1$) and lean mixtures with $\lambda \geq 2$. In the first configuration the maximum theoretical power is produced but with high NO_x production, while the second has extremely low NO_x emissions with an approximate power sacrifice of 40% (Verhelst & Wallner, 2009, Fig. 19). To counteract power losses when working with lean mixtures in port fuel injection systems (PFI), some researchers used superchargers, turbochargers, dual VVT, hybrid-electronic assistance, or a combination of the above; whereas, those who opted for stoichiometric mixtures used a reducing catalyst to reduce NO_x emissions. (Verhelst & Wallner, 2009; Verhelst, 2014)

Table 4
Influence of the richness of the mixture over performance in PFI-H2-ICEs

#	Vehicle	λ	Additional settings	Results
1	MAN H2876 UH01 12.8L 6L	1	Solenoid / sequential injectors	Maximum theoretical power density (86% of the gasoline version) Brake Thermal Efficiency BTE = 31%, EURO 5 emissions with reduction catalyzer, $r < 7.5$ to avoid abnormal combustion.
2	-	1.1	-	Highest burned gases temperature/ not highest NOx (lack of oxygen)
3	-	1.3	-	Maximum NOx
4	Ford P2000 (Zetec 2L 4L) $r=14.5$	1.8	-	18% better fuel consumption than gasoline counterpart, TLEV standard reached without aftertreatment.
5	-	2	-	Maximum theoretical power output reachable: 50% of gasoline stoichiometric counterpart; 100% if 1 BAR boost is added, SULEV
6	Chevrolet Silverado 1500 HD 6L V8 $r=12.1$	2.5	Supercharged / intercooler	0.8 BAR boost. Maximum theoretical power output: 80% of naturally aspired gasoline stoichiometric counterpart.
7	-	3.3	-	Highest efficiency reachable, minimum heat loses.
		4.5	-	Incomplete combustion, indicated efficiency decrement
8	GM 454 (Chevrolet Big Bock) 7.4L V8 $r=8.5$	2-5	λ variable / Load controlled	20% increase in engine power output vs. carbureted version / backfire free operation / high influence of injection timing on low loads & speed Region

Table 5*Influence of the richness of the mixture over performance (continue)*

#	Vehicle	λ	Additional settings	Result
9	Ford H2RV 2.3L	Variable, lean mixture	Supercharged Drive-cycle simulation Supercharged + hybrid-electric simulation	3% fuel economy increased compared with $\lambda = 2$ fixed 80% NOx reduction compared with $\lambda = 2$ fixed 53% fuel economy increased vs. conventional powertrain $\lambda = 2$ 99% less NOx vs. conventional powertrain with variable λ
10	Ford Shuttle bus 6.8L V10	Variable, lean mixture	Supercharged + hybrid-electric simulation In-vehicle test	12% Better BTE vs. gasoline counterpart @ 1500 RPM, 2.62 BAR BMEP 30% reduction of acceleration time (0-35mph) vs. natural gas counterpart / near zero emissions

The authors cited in the previous paragraph propose that the optimal air-fuel ratio must be such that there is a balance between power, efficiency and low NO_x emissions. To have a broader understanding of the possible configurations, Table 4 and Table 5 summarize the different air-fuel ratio choices used on in-vehicle tests with port fuel injection (PFI) and the engine performance of each option. In addition, theoretical reference values of λ related to maximum power, efficiency, gas temperature and NO_x production have been included.

A third configuration is cited by Verhelst & Wallner (2009), combining a stoichiometric ratio for high loads, and $\lambda \geq 2$ for low loads, avoiding as far as possible the range of high NO_x emissions ($1 < \lambda < 2$). This configuration was used in a 6L V12 demonstration vehicle, the BMW hydrogen 7; emissions registered were 0.008g/mi NO_x, equivalent to 3% of the maximum emissions allowed for the SULEV class.

Table 5 shows two projects using supercharger to counteract the low density of hydrogen in order to get higher power density as well as keeping near zero emissions. The article also provides another solution to this peculiar characteristic of hydrogen; cryogenic-hydrogen PFI. This type of injection allows 16% more air mass to enter within the cylinder, so higher power output is obtained. If this last solution is chosen, special care must be taken over safety issues and characteristics of the storage facility. (Verhelst & Wallner, 2009)

Beyond the classical configurations mentioned above, a novel investigation includes an extended range of air-fuel ratios, with rich mixtures up to $\phi = 1.3$ ($\lambda = 0.77$). Mentioned article studies the optimal choice of three factors: air-fuel mixture, exhaust gases

recirculation (EGR) and ignition time; tests were carried out on a 0.5L, 9:1 single-cylinder spark-ignited hydrogen engine on 2500RPM constant speed. With power as primary optimization factor, results showed that rich mixes ($\phi = 1.3$) with reduced EGR levels (0-0.47%) and moderate ignition advance (5-10°CA bTDC) gave the best balance between power and NO_x emissions (8.99-9.06 kW with 343-362 ppm NO_x). (Jabbar, Vaz, Khairallah, & Koylu, 2016)

2.4.3. NO_x formation

Nitric oxide (NO) and nitrogen dioxide (NO₂) are the result of the oxidation of atmospheric nitrogen, usually grouped and called NO_x, being nitric oxide the predominant component. In fact, the maximum value for the ratio NO₂/NO is 2% for equivalence ratio of 0.85 in SI engines (Heywood, 1988). It's clear that the author refers to a gasoline engine.

Other research on lean-mixture natural gas two-stroke engine revealed that the behavior above mentioned is not true for lean conditions. For this, tests were done for a range of equivalence ratio of $0.68 < \phi < 0.78$ ($1.5 > \lambda > 1.3$) showing a NO₂/NO_x ratio of 1 (that means only NO₂ was present) for equivalence ratios leaner than 0.7 ($\lambda > 1.4$); this is caused due to a sharp decay of NO for leaner mixtures as NO₂ emissions decreases with a smoother trend. (Olsen, Kohls, & Arney, 2010)

Focusing again on the fuel of interest in the present project, hydrogen, one can get the NO₂/NO ratio from fig. 14 on Homan, de Boer & McLean (1983). On their paper the

authors reported graphically NO and NO_x emissions for a wide range equivalence ratio ($0 < \phi < 1.3$). For an equivalence ratio of 0.5 ($\lambda = 2$; $NO_x \approx 100ppm$) NO₂/NO ratio is shown around 0.2 and increases for mixtures leaner than 0.3 equivalence ratio ($\lambda = 3.3$). Anyway, as mentioned on 2.4.2, it has been demonstrated that NO_x emissions are near zero for hydrogen engines working lean $\lambda \geq 2$.

One point more that needs to be considered is that nitric oxide (NO) is formed throughout the high-temperature burned gases behind the combustion flame and its highly temperature dependent; the higher the burned gases temperature, the higher the NO production rate is. (Heywood, 1988)

2.4.4. Engine parameters influence over performance

2.4.4.1. Ignition timing

As on every engine, the optimal ignition timing to get the best efficiency depends of the richness of the mixture, so an ignition map in function of the load is required for it. MBT (minimum advance for best torque) is the common setup of the engine companies, while represents the compromise between high power output and minimum ignition advance to decrease NO_x emissions (Sierens & Verhelst, 2000). However, as NO_x are greatly influenced by the ignition timing, another alternative usually used is to retard the ignition from MBT until torque is reduced 1 or 2 percent to decrease the toxic emissions (Heywood, 1988).

2.4.4.2. Injector placement

Chintala & Subramanian says combustion efficiency increases when the mixture formation gets more homogeneous and state for gaseous fuels the mixing process is more critical than with liquid fuels due to its lower density and lesser fuel penetration, even though its high diffusivity. In this way, to ensure a better mixing the injector placement is recommended not to be as closed as possible to the cylinder, but to be settled at some centimeters far from it to allow a larger mixing time within the inlet port. (Chintala & Subramanian, 2013)

2.4.4.3. Injection pressure

Is known power output is higher for a higher injection pressure for a fixed injection duration (Sierens & Verhelst, 2000). Due to the fact that injection pressure is a fixed value also, reported research usually use it like a setting; 2 or 3 bar are the popular choices. Nonetheless, for lean mixtures injection pressure can be optimize depending on the desire power output (Sierens & Verhelst, 2000).

2.4.4.4. Injection duration

Sierens and Verhelst, (2000) stated for injection-controlled load (qualitative load control) the injection duration must be proportional to the engine load; that means, the injection map must be linearized.

2.4.4.5. Injection timing backfire-free setup on PFI

As mentioned before on 2.3.2, and due to the extremely low minimum ignition energy of the hydrogen, injection timing has to be limited in order to avoid backfire. In this way, the start of the injection on hydrogen internal combustion engines is usually set some degrees after intake valves opening in order to have a pre-cooling time with fresh air to eliminate "hot spots", while the end of the injection has to take place before the intake valve closes to avoid hydrogen leftovers within the intake port that may lead to backfire in the next cycle (2009).

Nonetheless, it has been proved that backfire also depends on the compression ratio of the engine. To get to this conclusion tests were run on a single cylinder hydrogen engine where lower compression ratios presented a less flexible range of SOI possibilities. To be more precisely, the earliest Start of Injection to get a backfire-free operation was found to be 40, 30 & 20°CA aTDC for compression ratios of 4.5, 6.5 and 7.2 respectively, for an equivalence ratio of 0.7 ($\lambda \approx 1.7$). In addition, the authors remark backfire-free operation depends also on other parameters including engine speed, location of the injectors and engine load. (Salvi & Subramanian, 2016)

However, other authors have reported working with lean mixtures ($\lambda \geq 2$) to be a solution to ensure a backfire-free operation (Sierens & Verhelst, 2000). As a personal conclusion, based on the literature review mentioned above, a good procedure to find the backfire-free operation would be to start the injection relatively late, i.e. 50°aTDC, being sure the end of injection happens before the intake valve closes. After that, one should be

able to advance the injection carefully depending on the compression ratio, the equivalence ratio and the distance from the injector to the intake valve.

2.4.4.6. Influence of Injection Timing over performance

Sierens & Verhest, found that injection timing has a great impact for low speed and low loads for lean mixtures, with variations on the power output of even 20%, where the optimum range of Start of Injection was found to be at or before Top Dead Center (gas exchange) and needs to be advanced further for higher speeds. A GM/Crusader V-8 engine was used for the reported results, with hydrogen supplied from 200bar compressed tanks, further reduced to 3bar of injecting pressure, and delivered into the intake port of each cylinder individually. (Sierens & Verhelst, 2000)

Furthermore, some CFD simulation projects have also studied this phenomenon. Wang et. al (Wang, et al., 2017) studied the space distribution characteristics, velocity and turbulent kinetic energy under different injection timings for stoichiometric mixtures. A big range of possibilities were covered by the research, changing the Start of Injection from 370 to 510°CA in steps of 20°CA. Injection duration of 45°CA and ignition timing of 11°bTDC (709°CA) were used as fixed values. The results shown that only the first 5 groups (370-450°CA) were able to completely drive all the hydrogen inside as the others had some trapped hydrogen in the intake port. The uniformity of the mixture was also better for first 4 groups (370-430°CA) as late SOI shown to have a poor mixing (*Figure 1*).

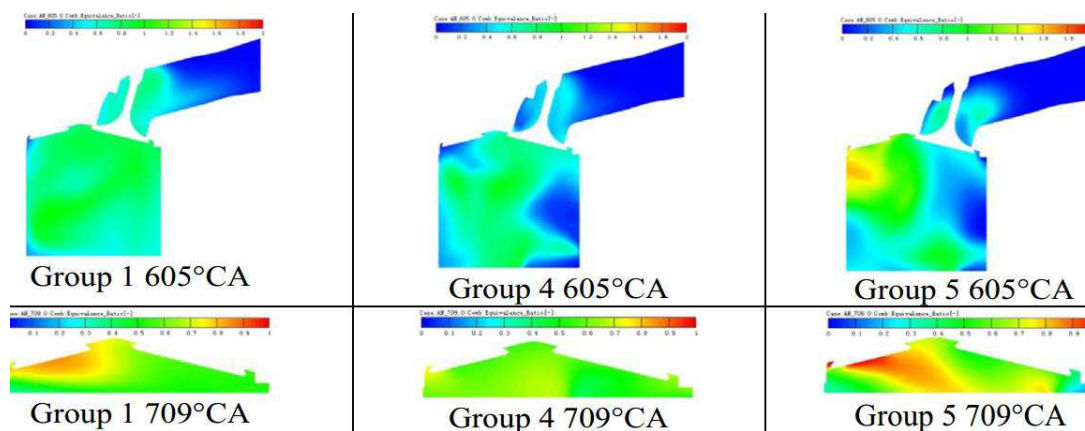


Figure 1. Equivalence ratio distribution under different SOI.

Font: (Wang, et al., 2017)

Other studies about injection timing has been done on H₂-DISI engines; higher indicated work and exponential decay of NO_x emissions were found for early SOI for lean mixtures. (Sierens & Verhelst, 2000; Nemati, Fathi, Barzegar, & Khalilarya, 2013)

2.4.4.7. Load control: throttle valve or injection control

Verhelst et. al state two load control possibilities for hydrogen engines: quantitative and qualitative. Quantitative load control refers to the regulation of the air by a throttle valve on the intake, while keeping a constant air-to-fuel ratio (commonly used on gasoline engines). Qualitative load control refers to the regulation of the amount of fuel injected, avoiding the need of a throttle valve, thus throttle losses. (Verhelst, et al., 2012)

2.4.4.8. Equivalence ratio

As said before, equivalence ratio has a great influence on the power output as on the NOx emission level. As shown on Table 4, a stoichiometric setting gives the higher power density (86% of a stoichiometric gasoline engine), while NOx emissions are 3000 ppm approximately, so a catalyzer is needed. By the other hand, working lean ($\lambda \geq 2$) produce near zero NOx but with a significant power penalty (maximum 50% of a stoichiometric gasoline engine). Equivalence ratios between $1 < \lambda < 2$ should be avoid in any case due to the existence of NOx production peak within this range. (Verhelst & Wallner, 2009)

2.4.4.9. Boost

In order to compensate the power penalty of working lean while keeping near zero NOx, 1 Bar boost supercharged setup is usually used. In this way, for $\lambda = 2$ the power density of the hydrogen PFI engine is the same as a stoichiometric natural aspiration gasoline engine (Verhelst & Wallner, 2009). Other projects directed by Tokyo City University and the University of Melbourne reported also successful results using turbocharged PFI H2ICE (Verhelst, 2014).

2.4.4.10. EGR

Exhaust gas recirculation have been reported to be a better NO_x emissions reduction strategy compared to retarded spark timing. Results of 50% emission reduction has been reported by using 20% EGR (Salvi & Subramanian, 2016)

CHAPTER III

THERMIC DESIGN

3.1. DEFINITION OF THE ENGINE OPERATING CONDITIONS

The work settings of the engine are established on Table 6. On Table 7 the sensors to be used and the measurement equipment is mentioned. In addition, this research is limited to the following:

- The engine will be provided by E. Van Wingen nv and no physical modification will be done. The engine in question is a naturally-aspirated, spark-ignited, 4 cylinders in line, 1.8 liters internal combustion engine with coil-on-plug ignition, coupled to a 4-poles LSES160L Leroy Somer asynchronous generator that has already been converted to work with hydrogen as fuel.
- In-cylinder pressure and temperature will not be measured.
- The useful heat of the engine will be determined through thermodynamic balance from the fuel flow, exhaust gases temperature and electric power output data.
- Heat losses to the environment will be assumed based on the literature review.
- Exhaust gases temperature will be measured through 4 thermocouples; one in each exhaust pipe of each cylinder.

- The hydrogen mass flow will be measured with a Bronkhorst EL-FLOW F-113AC sensor.
- An AEM EMS-4 ECU will be used to control the engine settings.
- Generated electricity must match the requirements of Ghent University laboratory's grid; 380V and 50Hz.

Table 6
Work settings

Settings	
Air intake	WOT – No boosted
Speed	2500 RPM
Fuel control	Quantitative
Air control	WOT
Load control	Electronic (0 to 5V)
	Ethylene glycol
Refrigeration	50%
Carter ventilation	Positive
Exhaust gases treatment	None
Exhaust gases recirculation	Not available

Note: WOT: Wide open throttle.

Table 7
Sensors and measurement equipment

Variable	Type	Accuracy
Air flow	No sensor	
Fuel mass-flow	Bronkhorst F-113AC-HD-00-V	0.9 %FS
Exhaust gases temperature	Four K-type TC / 1 per cylinder outlet	$\pm 2.2^{\circ}\text{C}$ or $\pm .75\%$
Electric power output	Socomec Diris A40	$\pm 0.01\text{kWe}$
NO emissions	Maihak UNOR 610	1%
Oxygen on the exhaust	Sick-Maihak OXOR S710	1%
Unburned hydrogen on the exhaust	Maihak THERMOR S710	1%
Air-fuel ratio	Bosh LSU 4.9 lambda sensor	± 0.05 at $\lambda = 1.7$
In-cylinder pressure	Not available	-
Coolant temperature	K-type TC	$\pm 2.2^{\circ}\text{C}$ or $\pm .75\%$
Coolant flow	Not available	-

3.2. BASELINE OF THE PROJECT

As it was said before, the engine available at UGent was a natural gas engine, part of a CHP unit, that was converted into hydrogen operated ICE. The engine is connected to a 15kW generator and the load is simulated through an external power supply of 5 Volts, being 5 Volts full load. Is also important bear on mind that the load in a CHP unit is the percentage of the maximum power that the generator could send to the grid; in this way,

for the configuration established before, no-load means that no power is supplied from the engine to the grid, and full load means 9kWe is provided from the engine to the grid.

In addition, E. Van Wingen nv, the promoters of the project, has also another engine, with the very same characteristics as the one on UGent, being tested on Antwerp, sponsored by Air Liquide Industries. The results from the CHP on Antwerp will be used to validate the estimations obtained with the engine on UGent.

So, going back to the fact that there are two identical engines connected to identical generators, one on UGent with a fan-radiator for the cooling system and no heat exchanger on the exhaust pipe, while the one on Antwerp has a three-heat-exchangers system as shown on *Figure 2*, the control volume for the thermodynamic analysis was set as the generating group, engine plus generator, as shown on *Figure 3*. This control volume was chosen in order to test the two engines on the same conditions, and in that way, getting the base efficiencies and power-to-heat ratio of the CHP unit.

In order to be considered as the same control volume, both engines were set with the same ECU and ECU's mappings and settings, and same generator. The combustion thus, is reproduced under the same conditions. The influence of the environmental conditions was assumed to be negligible.

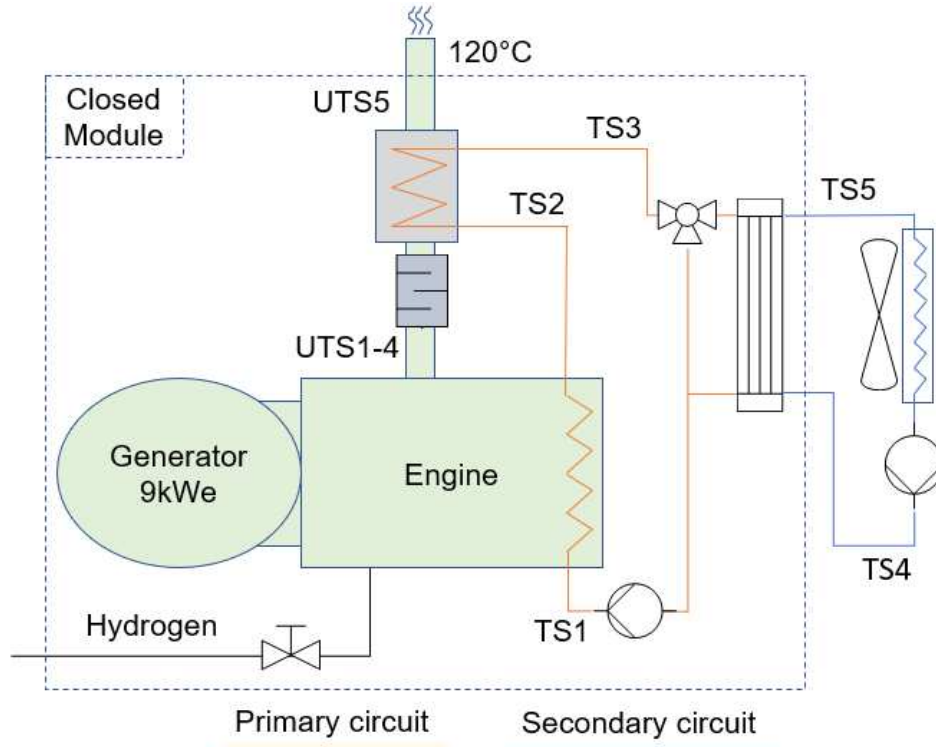


Figure 2. Layout of the CHP unit configuration.

$$(\dot{m}_f)_{Antwerp} = (\dot{m}_f)_{UGent} \quad (3.1)$$

$$(\dot{E})_{Antwerp} = (\dot{E})_{UGent} \quad (3.2)$$

$$(\dot{H}_{exh})_{Antwerp} = (\dot{H}_{exh})_{UGent} \quad (3.3)$$

$$(\dot{Q}_{cool} + \dot{Q}_{losses})_{Antwerp} = (\dot{Q}_{cool} + \dot{Q}_{losses})_{UGent} \quad (3.4)$$

3.2.1. Global heat balance

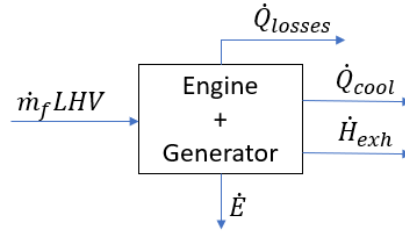


Figure 3. Heat Balance on the generating group.

$$\dot{m}_f \cdot LHV = \dot{E} + \dot{H}_{exh} + \dot{Q}_{cool} + \dot{Q}_{losses} \quad (3.5)$$

$$\dot{H}_{exh} = \dot{Q}_{HEX_{exh}} + \dot{Q}_{condenser} + \dot{H}_{waisted}, \quad \dot{Q}_{condenser} = 0 \quad (3.6)$$

$$\dot{Q}_{HEX_{exh}} = \dot{m}_{exh} \cdot c_{p_{exh}} \cdot (\bar{T}_{exh} - UTS5), \quad UTS5_{design} = 120^\circ C^{23} \quad (3.7)$$

$$\bar{T}_{exh} = \frac{UTS1 + UTS2 + UTS3 + UTS4}{4} \quad (3.8)$$

$$\dot{Q}_{cool} = \dot{m}_{et1} \cdot c_{p_{et1}} \cdot (TS2 - TS1) \quad (3.9)$$

The engine at Antwerp takes the heat power from the exhaust only till the temperature drops down to 120°C. To improve the system's efficiency a condenser must be installed on the secondary circuit, after the Heat Exchanger but before the Fan. The heat power of the condenser can be represented by the formula bellow taking on account T_{exhout} has to be over the dew point of the exhaust gases to avoid the rapidly deterioration of the system; the calculated dew point occurs at 63°C for lambda 2.

²³ Data taken from Van Wingen P&ID of the Mini-WKK for Natural Gas.

$$\dot{Q}_{condenser} = \dot{m}_{exh} \cdot cp_{exh} \cdot (UTS5 - T_{exhout}) \quad (3.10)$$

3.2.2. Coolant properties

The properties of the Ethylene Glycol correspond to the next formula:²⁴

$$cp_{et} = A + BT + CT^2 \quad (3.11)$$

Where A=0.81485, B=7.3219E-4, C=0 for 50% of concentration.

3.2.3. Fuel power

The fuel power F is calculated as means of the measured hydrogen mass flow \dot{m}_f multiplied by the Lower Heat Value of the fuel LHV .

$$F = \dot{m}_f \cdot LHV \quad (3.12)$$

3.2.4. Thermal power available for recovery

The thermal power available for recovery \dot{Q}_{rec} is calculated by subtracting the unavoidable losses \dot{Q}_{losses} and the electrical power generated divided by the generator's

²⁴ Font: (MEGlobal, 2008).

efficiency \dot{E}/η_{gen} from the fuel power F . The unavoidable losses are assumed to be a percentage of the fuel power ($\dot{Q}_{losses} = X_{disp} \cdot F$).²⁵

$$\dot{Q}_{rec} = F - \dot{E}/\eta_{gen} - \dot{Q}_{losses} \quad (3.13)$$

$$\dot{Q}_{rec} = \dot{H}_{exh} + \dot{Q}_{cool} \quad (3.14)$$

3.2.5. Thermal power available on the exhaust gases

$$\dot{H}_{exh} = \dot{m}_{exh} \cdot c_{p_{exh}} \cdot \bar{T}_{exh} \quad (3.15)$$

$$\dot{H}_{exh} = \dot{Q}_{HEX_{exh}} + \dot{Q}_{condenser} + \dot{H}_{waisted} \quad (3.16)$$

From the mass conservation at a control volume

$$\dot{m}_{exh} = \dot{m}_{in} \quad (3.17)$$

The mass flow on the intake was get from the fuel mass flow and the lambda value, both measured.

$$\dot{m}_{in} = \dot{m}_f + \dot{m}_a \quad (3.18)$$

$$\lambda = \frac{AFR}{AFR_s} \quad (3.19)$$

$$AFR = \frac{\dot{m}_a}{\dot{m}_f} \quad (3.20)$$

²⁵ X_{disp} was assumed as 5% in Caresana, Brandoni, Feliciotti, & Bartolini, (2011) & in Table 4 of Radu, Micheli, Alessandrini, Casula, & Radu (2015). Jadhao & Thombare, (2013) said that 5% fuel energy is lost as radiation.

$$\dot{m}_a = AFR \cdot \dot{m}_f \quad (3.21)$$

$$\dot{m}_a = \lambda \cdot AFR_s \cdot \dot{m}_f \quad (3.22)$$

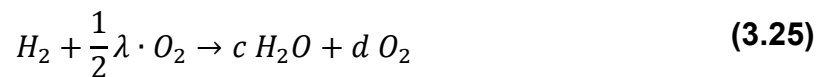
$$\dot{m}_{exh} = \dot{m}_{in} = \dot{m}_f(1 + \lambda \cdot AFR_s) \quad (3.23)$$

3.2.6. Hydrogen combustion – chemical equation

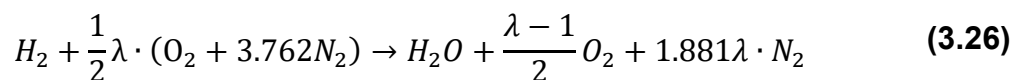
The complete theoretical equation of the hydrogen combustion is:



By adding excess of air in means of the air-to-fuel equivalence ratio:



Where $d = (\lambda - c)/2$ and $c = 1$. The equation of real combustion with excess of air is as follows:



3.2.7. Properties of the exhaust gases

The exhaust gases enthalpy was calculated by mole fraction from the chemical equation of the hydrogen real combustion with excess of air as it's suggested in McAllister, Chen & Fernandez (2011, p. 41). To determine the mole fraction, the total number of

moles, N , must be determined from the chemical equation. This value is the addition of the number of moles of each component of the mixture:

$$N = \sum_{i=1}^k N_i \quad (3.27)$$

Where N_i is the number of moles of species i in the system. From that, the mole fraction is

$$y_i = \frac{N_i}{N} \quad (3.28)$$

The average molar mass in means of mole fraction is determined by

$$M = \frac{m}{N} = \frac{\sum_i N_i M_i}{N} = \sum_i y_i M_i \quad (3.29)$$

Having these values, the enthalpy of a mixture, h (kJ/kg), can be determined by

$$h = \frac{1}{M} \sum_{i=1}^k y_i \cdot \hat{h}_i \quad (3.30)$$

where i refers to the species, y_i is the mole fraction of species i , M is the average molecular mass of the mixture in mole fraction basis and $\hat{\quad}$ indicates that a quantity is per mole. The sensible enthalpy as well as the total enthalpy in mole basis are defined as

$$\hat{h}_{si} = \int_{T_0}^T \hat{c}_p(T) dT \quad (3.31)$$

$$\hat{h}_i = \Delta \hat{h}_i^0 + \hat{h}_{si} \quad (3.32)$$

where the subscript i refers to species i , h_s to sensible enthalpy, Δh^0 to enthalpy of formation at standard condition (25°C & 1atm) and T_0 to standard temperature (25°C).

Note that, if phase change happens, the total enthalpy needs to include the latent heat:

$$\hat{h}_i = \Delta\hat{h}_i^o + \hat{h}_{si} + \hat{h}_{latent}$$

For water, the latent heat of vaporization is $\hat{h}_{fg} = 40.65 \text{ kJ/mol}$ at 100°C & 1atm ; latent heat of the oxygen and nitrogen are not considered due to their very low boiling point of -183 and -195.8 degrees Celsius respectively (see Table 9). The enthalpy of formation of elements in their most stable forms, as N_2 and O_2 , is zero, while for $H_2O_{(g)} = -241.83 \text{ MJ/kmol}$. (McAllister, Chen, & Fernandez-Pello, 2011, p. 24)

Table 8
Enthalpy of formation of common combustion species

Species	$\Delta\hat{h}_i^o$ [MJ/kmol]	Species	$\Delta\hat{h}_i^o$ [MJ/kmol]
H ₂ O(g)	-241.83	H	+217.99
CO ₂	-393.52	N	+472.79
CO	-110.53	NO	+90.29
NO	+90.29	NO ₂	+33.1
NO ₂	+33.1	O	+249.19
N ₂ , O ₂	0	OH	+39.46

Note: Selected data from McAllister, Chen, & Fernandez-Pello, 2011, p. 25, Table 2.2.

Table 9
Latent heat of common products of hydrogen combustion

Species	\hat{h}_{latent} [kJ/kmol]	Boiling point [$^\circ\text{C}$]
H ₂ O(g) ^b	40660.5	100
Nitrogen ^b	2792.8	-195.8
Oxygen ^b	3409.9	-183
NO ^a	13.8×10^3	-151.7
NO ₂ ^a	38.1×10^3	21

Note: Molar latent heat was calculated from the molar weight and the latent heat on kJ/kg. ^a(Vargas, 2011) ^b(Cengel, 2011).

CHAPTER VI

EXPERIMENTAL TESTS OF ENGINE-SETTINGS INFLUENCE OVER POWER AND EMISSIONS

4.1. EXPERIMENTAL DESIGN

Table 10
Experimental investigation planning

Parameter	Injection	Spark	Pressure	Lambda	Electric
Test	Timing	Timing			Power
First phase: effect of engine factors over power distribution					
Injection	370 –	Fixed at	Fixed on 2	Fixed:	-
Timing	410°CA step:10°CA	11°bTDC	bar	2, 2.1, 2.2.	
Spark	Fixed on	3°aTDC –	Fixed on 2	-	9kW
Timing	BRoPT	21°bTDC	bar		
Pressure	Fixed on	MBT:	1.5 – 2.5	-	9kW
	BRoPT	BRoPT	bar		
Second phase: part load and higher power					
Part load	Fixed on	Fixed on	Fixed on	-	5 &
performance	BRoPT	BRoPT	BRoPT		7.5kW
Increasing	Fixed on	Optimum	Fixed on	-	MPbEL
load	BRoPT	range	BRoPT		
Third phase: mapping possibilities					
	MBT ST mapping		Minimum NOx at higher power map		

Note: BRoPT: Best Result of Previous Test. MPbEL: Maximum Power below Emissions Limit.

As established before, the engine will not be physically modified and, based on the literature review, by changing the engine parameters controlled by the ECU good results can be obtained. In this way engine parameters to be tested are: ignition timing, injection timing and pressure. Lean mixtures were chosen in order to get the lowest emissions possible; the regulation limits exposed in 2.2.3 were taken as reference. Wide Open Throttle (WOT) configuration was chosen to avoid throttle losses. Finally, the experimental tests planning is shown in Table 10.

4.2. EFFECT OF ENGINE FACTORS OVER POWER DISTRIBUTION

4.2.1. Start of Injection

4.2.1.1. Test settings

Based on the established by Sierens & Verhelst (2000) and confirmed in the CFD study by Wang et. al (2017), early Start of Injection (SOI) was chosen as has been proved to be the best configuration. SOI of 370-410 degrees of crank angle ($^{\circ}\text{CA}$), in steps of 10°CA were taken as the options to be tested, starting on 410°CA and advancing the SOI carefully in order to avoid the backfire zone if existent. As an additional safety procedure to avoid enclosed high pressures due to a possible backfire, the metal clamp of the air intake pipe was loosened, so the extra pressure was able to make its way out without any severe damage to the intake manifold. Results were evaluated for lambda values of 2, 2.1, and 2.2. Ignition timing was fixed on 11°bTDC as it represents MBT at lambda 2.

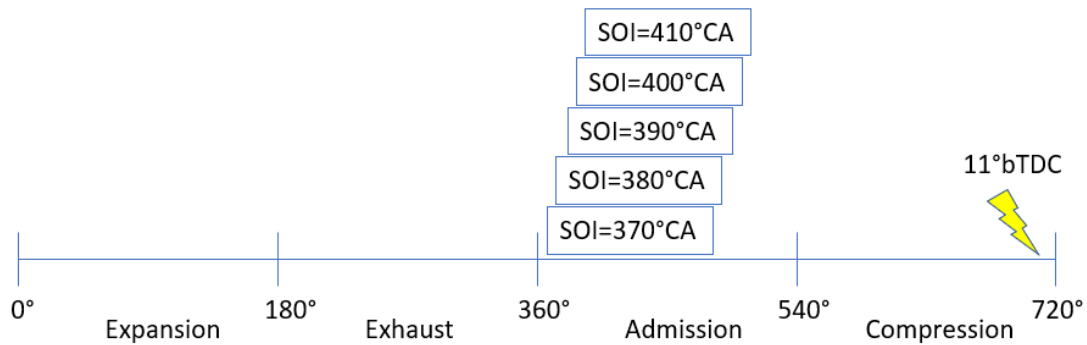


Figure 4. Start of Injection test settings.

4.2.1.2. Electric Power

As can be seen on *Figure 5*, electric power showed not to have the same trend on the three curves, but to have a different behavior depending on the richness of the mixture. For lambda 2 for example, 1.3% (0.12kW) higher power was reached by advancing the SOI from 410 to 390°CA, while for lambda 2.2 the trend was the opposite for the same SOI compared before. In this way, the highest electric power output SOI was 390 and 410°CA for lambda 2 and 2.2 respectively, in contrast with lambda 2.1, in which electrical power kept constant all the way.

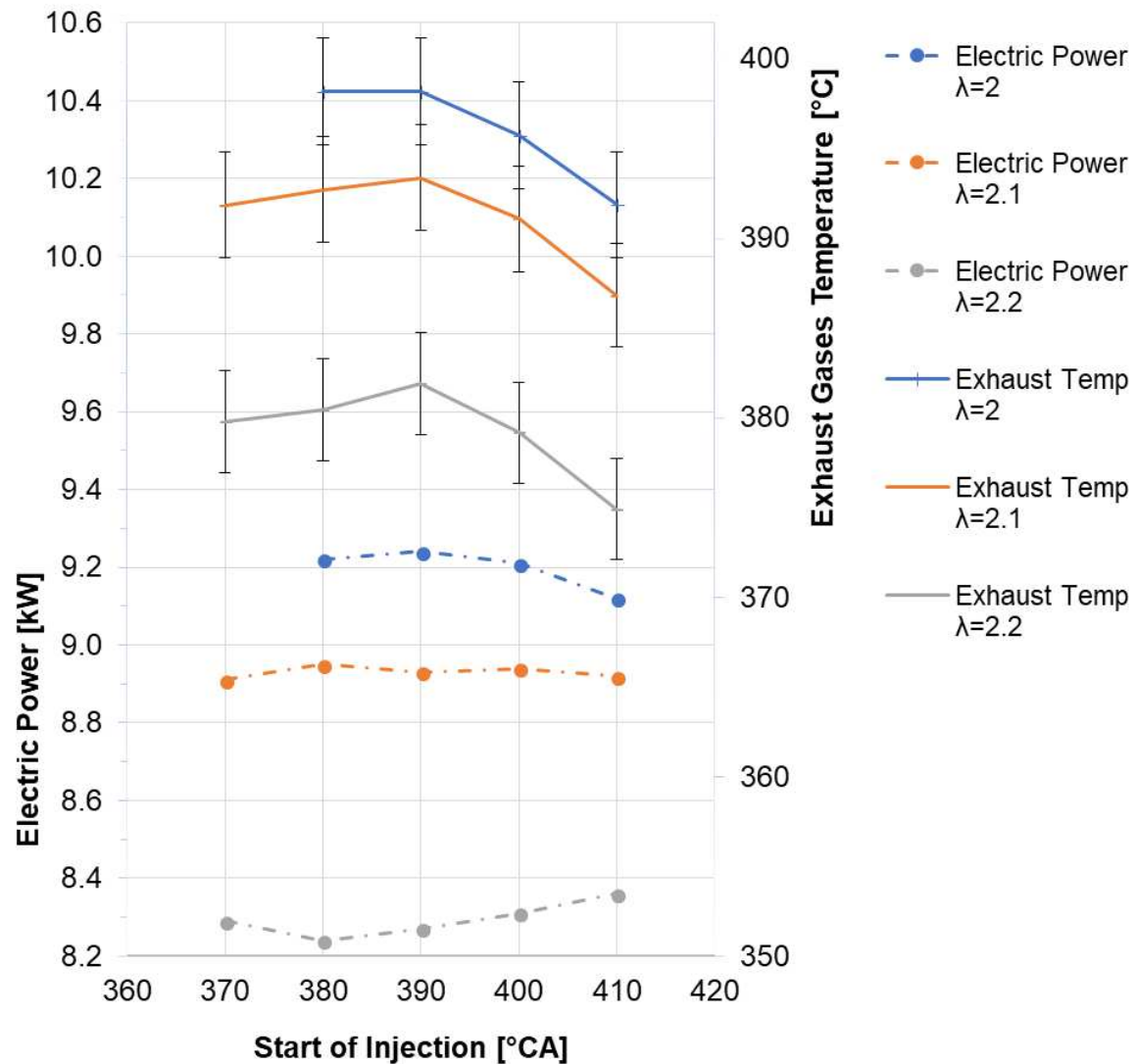


Figure 5. Electric Power & Exhaust Gases Temperature vs. Start of Injection.
 Note: ST=11°bTDC, 2 BAR injection pressure.

4.2.1.3. Exhaust Power

For all lambda settings, SOI that corresponds to the higher exhaust power was 390°CA, while the lowest was 410°CA. The influence of changing the SOI was smoother for richer mixtures. The maximum difference was found at lambda 2.2, showing 3% higher exhaust

thermal-power available (0.24kWth) on SOI=390 vs SOI=410°CA due to a 7°C gap of exhaust gases temperature.

4.2.1.4. NO emissions

Differing with electric and heat power, NO emissions were found to be highly affected by the injection timing. *Figure 6* shows NO emissions kept steady from 370 until 390°CA but increased for later SOI; this behavior is sharper notable for richer mixtures. It's also notable in *Figure 6* that NO emissions related with later start of injection are even above the NOx limit; this may due to insufficient time to get a completely homogeneous mixture even when one can argue that being such early injection hydrogen must have enough time to get well mixed with air. Anyway, as mentioned on 2.4.4, the CFD simulation done by Wang et. al (2017) supports this theory.

4.2.1.1. Fuel consumption

The fuel consumption shown to be constant according to the amount of fuel.

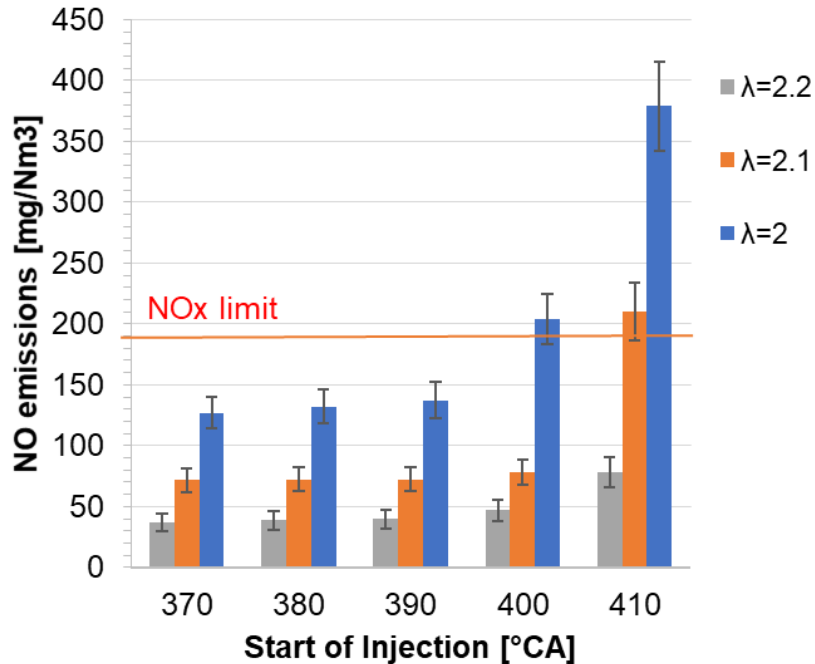


Figure 6. NO emissions vs. start of injection.
 Note: ST=11°bTDC, 2 BAR injection pressure.

4.2.1.2. Results

In order to keep the lowest NOx emissions possible, SOI needed to be set at or before 390°CA (30°aTDC of gas exchange). Taking about power distribution, for this range (SOI≤390°CA), both, the electrical power and the heat power kept with similar values, with less than 1% of variation (0.05kW); for both, the best configuration was found to be at SOI=390°CA. Nonetheless, as the engine required to be optimized at 9kW and may look for higher electrical power output on future tests, 380°CA was chosen as the optimal configuration in order to have a wider injection-duration flexibility range without compromising the performance of the engine.

In addition, an important point to be mentioned is the fact that, in contrast with one may think, later start of injection produced higher NO emissions while the exhaust gases temperature was lower than for earlier SOI. Starting on the fact that NO production is highly temperature dependent and is higher for higher temperatures, the possibility of producing more NO and lower exhaust gases temperatures at the same equivalence ratio may sounds crazy at first glance. Anyway, this circumstance may be caused by a faster combustion process due to the inhomogeneity of the mixture. In this way, NO production may be higher due to the higher temperature of the flame in the richer mixture zone while exhaust gases do not gain too much heat due to the higher flame velocity related to that zone. A similar behavior was found for injection pressure test, mentioned in 4.2.3.

4.2.2. Ignition Timing

4.2.2.1. Test settings

Test were done by changing the ignition timing for a fixed electric power of 9kW. The procedure was to retard the ignition timing and compensate the electrical power decrease by increasing the load. A big range was chosen in order to have a better picture of the possibilities and its limitations Ignition timing from 21°bTDC to 3°aTDC were tested by steps of 3°CA; additional measurements were done around MBT. The tests were done with Start of Injection at 380°CA.

4.2.2.2. Emissions & fuel consumption

Figure 7 shows the fuel consumption, NO emissions and temperature of the exhaust gases for the range of ignition (or spark) timing mentioned above. For better comprehension, the figure was divided into four zones; each zone is further analyzed in. By the other hand, zone IV needs to be avoided in any case due to a quick increase of NO emissions, even over the limit of NO_x establish by the VLAREM II. Zone I also needs to be avoided as it's consider to be too far retarded, showing even more a decay on the rate of temperature rise of the exhaust gases per °CA; this decay may be caused by a decrease of fuel-consumption increasing-rate.

In any case, since the best balance between better fuel consumption and lower NO is the common point of zones II and III, zone II was found to be the best working zone for an ICE-based CHP unit (as long as no electric storage or selling-to-the-grid configuration would be available). This zone encloses the highest rate of temperature rise per degree of crank angle as keeping NO emissions almost constant and far away from NO_x limit.

Table 11. Recommended zones for each characteristic were highlighted with green, while “to avoid” zones are on red. Coolant temperature was added in Table 3 as reference besides it may not be a decision-making factor.

Zone III is recommended for being a steady minimum fuel consumption zone, nonetheless, the best ST setting within the mentioned zone is for sure the lower NO emission point, in this case 10.5°bTDC. If more heat is needed to be produced, zone II is the best option due to a high rate of temperature rise of the exhaust gases per °CA retarded; 11.5% higher heat power on the exhaust was reached due to a 37.6°C

temperature increase by retarding ST from 10.5 to 0°bTDC. 6% higher fuel consumption was the price for this heat power increase.

By the other hand, zone IV needs to be avoided in any case due to a quick increase of NO emissions, even over the limit of NO_x establish by the VLAREM II. Zone I also needs to be avoided as it's consider to be too far retarded, showing even more a decay on the rate of temperature rise of the exhaust gases per °CA; this decay may be caused by a decrease of fuel-consumption increasing-rate.

In any case, since the best balance between better fuel consumption and lower NO is the common point of zones II and III, zone II was found to be the best working zone for an ICE-based CHP unit (as long as no electric storage or selling-to-the-grid configuration would be available). This zone encloses the highest rate of temperature rise per degree of crank angle as keeping NO emissions almost constant and far away from NO_x limit.

Table 11
Spark Timing zones characteristics

	Zone I	Zone II	Zone III	Zone IV
Fuel consumption (increasing rate)	Higher FC (-)	6% higher FC by retarding 10.5°CA (0.6%/°CA)	Steady / Minimum FC (-)	Increasing FC (-)
Exhaust Gases Temperature (increasing rate)	Increased 7.7°C by retarding 3°CA (2.6°C/°CA)	Increased 37.6°C by retarding 10.5°CA (3.6°C/°CA)	Increased 8.1°C by retarding 4.5°CA (1.8°C/°CA)	Steady (-)

CONTINUE 

NO emissions (increasing rate)	Statistically steady. Lower emission area (-)	24% lower NO by retarding 10.5°CA (3%/°CA)	39% lower NO by retarding 4.5°CA (9%/°CA)	Out of the NOx limit (n/a)
Coolant Temperature (increasing rate)	Increased 0.3°C by retarding 3°CA (0.1°C/°CA)	Increased 0.2°C by retarding 10.5°CA (-)	Increased 0.1°C by retarding 4.5°CA (-)	Increased 0.5°C by advancing 6°CA (0.1°C/°CA)

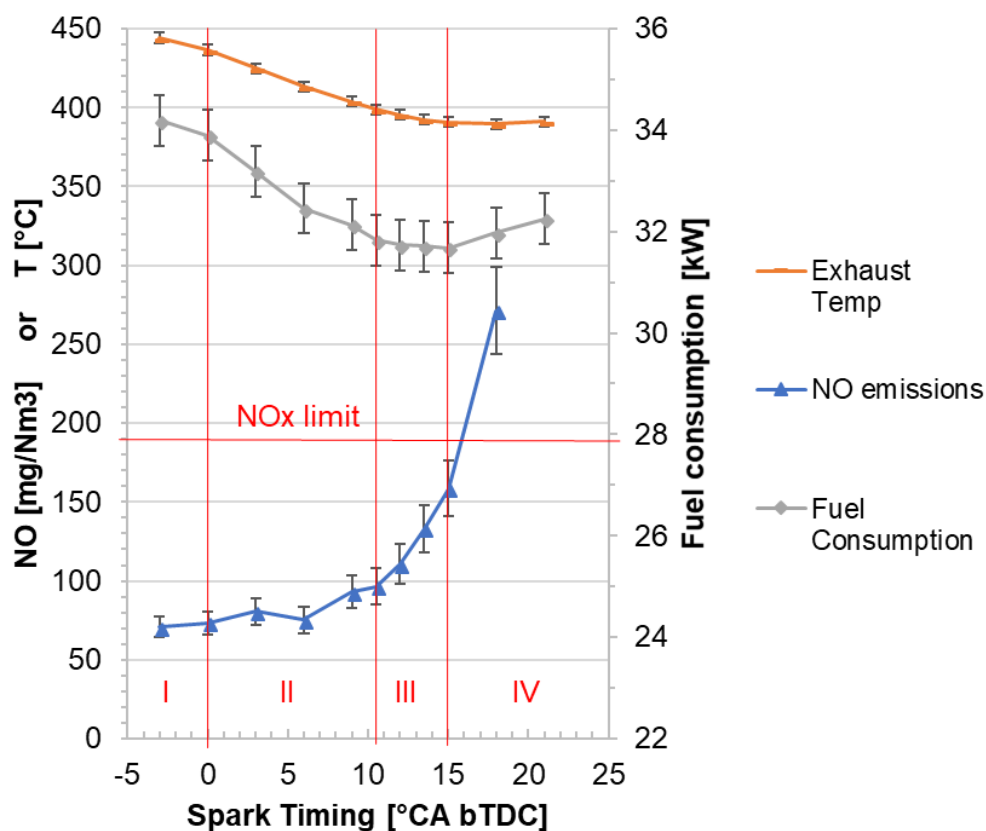


Figure 7. Performance curve at 9kW for various spark timing.

4.2.2.3. Electric Efficiency

As shown in *Figure 8*, maximum electric efficiency was 28.44% for 15°bTDC and dropped down to 26.35% by retarding 18°CA. Nonetheless, this 2% difference is not lost, but transformed into heat available. However, the fraction of thermal power available that can be taken as useful thermal power would rely on the design of the CHP heat exchangers system.

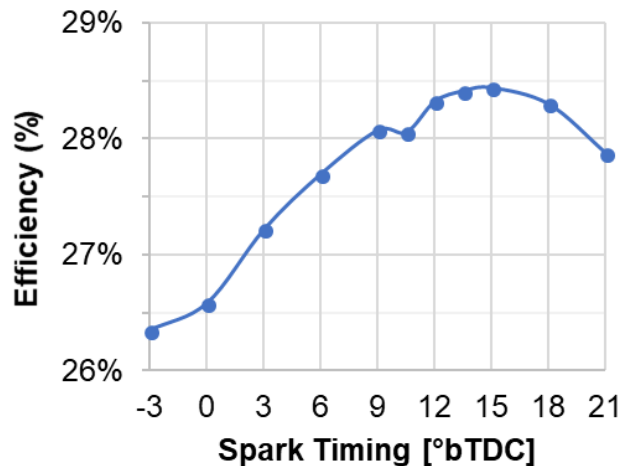


Figure 8. Efficiency of electrical power production.

4.2.2.4. Influence of Ignition Timing on useful power distribution

Figure 9 shows the share of fuel power of the engine. Electric power is 9kW constant, as the rest of the fuel power is divided into exhaust power available and coolant power available. The exhaust power available was calculated as $\dot{Q}_{exh} = \dot{m}_{exh} \cdot h$ from the equations established on Chapter 3. Only the sensible heat was considered as enthalpy

because the dew point of the water vapor fraction existent in the exhaust gases is usually avoided.

To calculate the heat power available on the coolant, the electric power divided by the generator efficiency, heat power available on the exhaust gases and heat losses were subtracted from the fuel power.

$$\dot{Q}_{cool} = F - \dot{E}/\eta_{gen} - \dot{H}_{exh} - x_{losses} \cdot F \quad (4.1)$$

The heat losses ($x_{losses} \cdot F$) are due to heat transfer from the engine block to the environment; 5% fuel power is assumed as done on both, Caresana, Brandoni, Feliciotti, & Bartolini, (2011) & Radu, Micheli, Alessandrini, Casula, & Radu, (2015). The efficiency of the generator (η_{gen}) is 90.6%.²⁶

4.2.2.5. Results

The heat of the exhaust gases was minimum for greater ignition advance, while the heat from the cooling system had the minimum power between 10 and 15°bTDC, the same range of the minimum fuel consumption (shown as a yellow line). While for a further advance of ignition timing the heat of the exhaust gases kept being the minimum, the heat from the cooling system rose due an increase of fuel consumption. 16.1% higher exhaust-gases heat available (1.3kW) was reached by retarding the ST from 15°bTDC to 3°aTDC due to an increase of 53°C on exhaust temperature. The coolant power available also

²⁶ The efficiency was taken from the generator catalogue (Leroy-Somer, 2018) p.69, for 380V 50Hz operation.

rose a 9.7% (1.2kW). In total, 2.5 kilowatts more are available as heat by retarding the spark timing 18°CA.

However, as established before on 4.2.2.2, to retard 18°CA is not the best choice to generate higher heat, as the engine is also under higher thermal load and also due to a diminished fuel economy. Repeating the analysis only for zone II (from 10 to 0 °bTDC), 11.5 (1.0kW), 7.6 (0.9kW) and 9.2 (1.9kW) percent higher heat power is available on the exhaust, coolant and as total heat respectively.

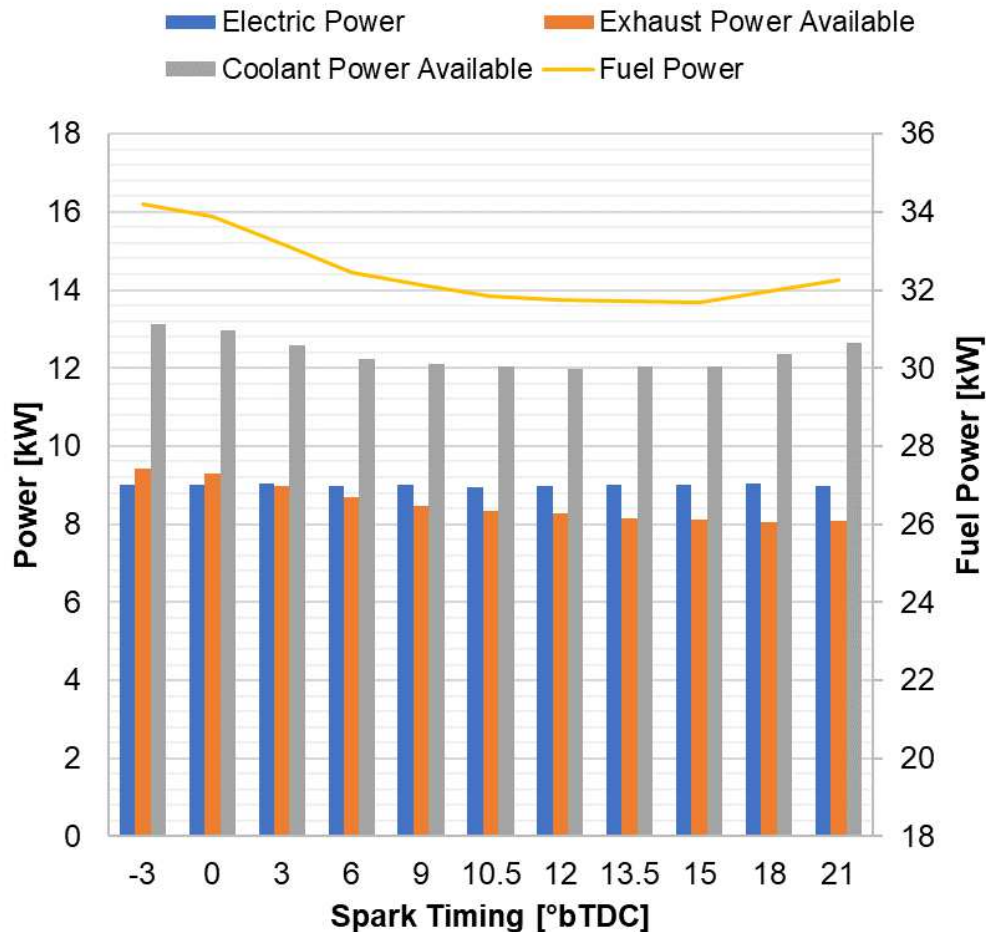


Figure 9. Influence of ST on power distribution at 9kWe.

4.2.3. Injection Pressure

4.2.3.1. Test settings

Injection pressure was tested between 1.5 & 2.5 bar in steps of 0.25 bar. In order to have a practical comparison of the data, the engine was fixed at full load (9kWe). To compensate the decrease of the power output due to a decrease of the injection pressure, the injection duration was increased by increasing the load, so differences of ± 0.1 kW were measured. SOI was fixed at 380°CA and Ignition timing was fixed on 10.5°bTDC , as it represents the optimal advance to get higher power without raising the emissions, defined also like the common point between zone II and III.

4.2.3.2. Exhaust temperature

The influence of injection pressure over exhaust gases temperature had a nonlinear decreasing behavior from 1.5 to 2.5 bar. Nonetheless, the maximum and minimum temperature were found at 1.75 & 2.25 bar. 2.2% more exhaust thermal-power available (0.2kWth) was found due to a rise of 7°C in the exhaust gases temperature comparing 1.75 & 2.25 bar results. By the other hand, temperature differences on the coolant at the outlet of the engine not higher than 0.2°C were registered on the measurements.

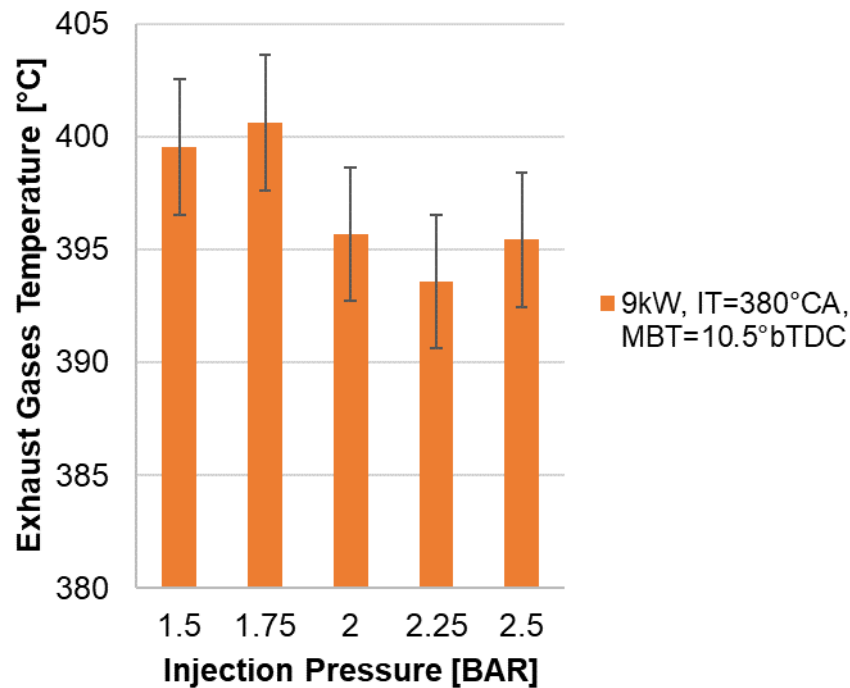


Figure 10. Injection pressure influence over exhaust temperature.

4.2.3.3. NO Emissions

On *Figure 11*, injection pressure influence over NO emissions is shown. A nonlinear increasing trend was found for higher pressures over the established range. A difference of 61% NO emissions was found for 2.5 bar comparing to 1.5 bar. A reduction of 36% emission was reached by lowering the pressure from 2 bar, that was the previous setting of the engine, to 1.5 bar.

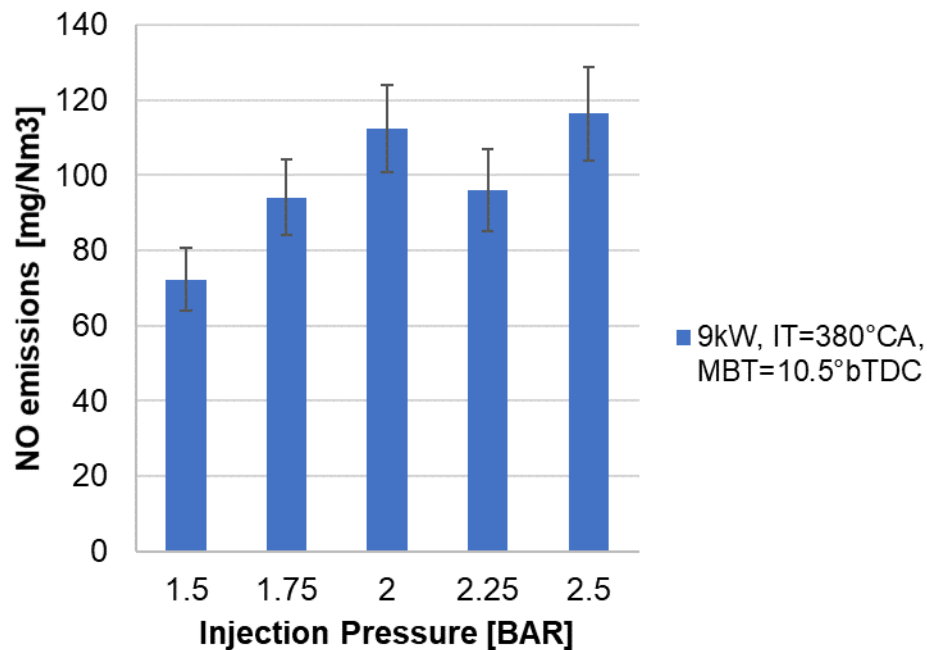


Figure 11. Injection pressure influence over NO emissions.

4.2.3.4. Fuel Consumption

The fuel consumption for 1.5, 1.75, 2, 2.25 & 2.5 bar was 10.70, 10.73, 10.75, 10.59 & 10.60 Nm³/h; at higher pressures the fuel consumption shown to be slightly lower. In any case, these results may be cause of the output power differences existent on the measurements as mentioned on the test settings established above (± 0.1 kW).

4.2.3.5. Results

To have a better analysis of the injection pressure influence over the performance of the engine fixed at full load (9kWe), 2 bar injection pressure was taken as the point of

reference as it was the previous pressure set on the engine. At injection pressures lower than 2 bar the exhaust gases temperature was higher while keeping the lowest NO emissions. By the other hand, higher pressures, 2 bar included, presented lower exhaust gases temperatures but higher NO emissions; this may be caused by a faster combustion process related with a slightly inhomogeneous mixture. A similar behavior was found for start of injection test and it is already explained on 4.2.1.

4.3. PART LOAD AND HIGHER POWER

Once optimized Start of Injection and Injection Pressure were found (Table 12), further tests were done changing spark timing to study the possibility of producing higher thermal power at part load and, step further, the possibility of reaching electric power outputs over 9kW under NOx limit. Total heat available, fuel consumption & electric efficiency for both, part load and higher power tests are shown down below on *Figure 12, Figure 13 & Figure 14*. Total heat available was calculated as the addition of the thermal power available on the exhaust gases and the thermal power available on the coolant.

Table 12
Baseline from the previous phase

Feature	Best configuration
Injection Timing	380°CA
Spark Timing Range	Zone II: MBT and retarded 10-12°
Pressure	1.5BAR

Note: MBT for 9kWe was 11°bTDC.

4.3.1. Thermal power available at part load

For the part-load study, a wide range of spark timing possibilities like done previously on 4.2.2 were tested at 5 & 7.5kW fixed electric power output.

At part load, 5 and 7.5kWe, NO emissions were constant over whole the testing range; 36.36 mg/Nm³ (28ppm) at 5kWe and 29.03 mg/Nm³ (31ppm) at 7.5kWe. Is important to notice emissions were higher at 5kWe in standard units (mg/Nm³) due to a higher amount of oxygen, 11.51%O₂ for 5kWe and 7.84%O₂ for 7.5kWe; this has a big influence when converting from parts per million (ppm) to milligrams per normal cubic meters (mg/Nm³). Anyway, both amounts kept constant and are too small to be a decision factor of the optimal spark timing on part load.

On *Figure 12* its shown the heat available flexibility for a fixed electric power output at part load. 17.83% (2.58kWth) higher heat available was reached at 5 electric kilowatts by retarding 27°CA. At 7.5kWe, 13.19% (2.33kWth) higher heat available was reached by retarding 21°CA.

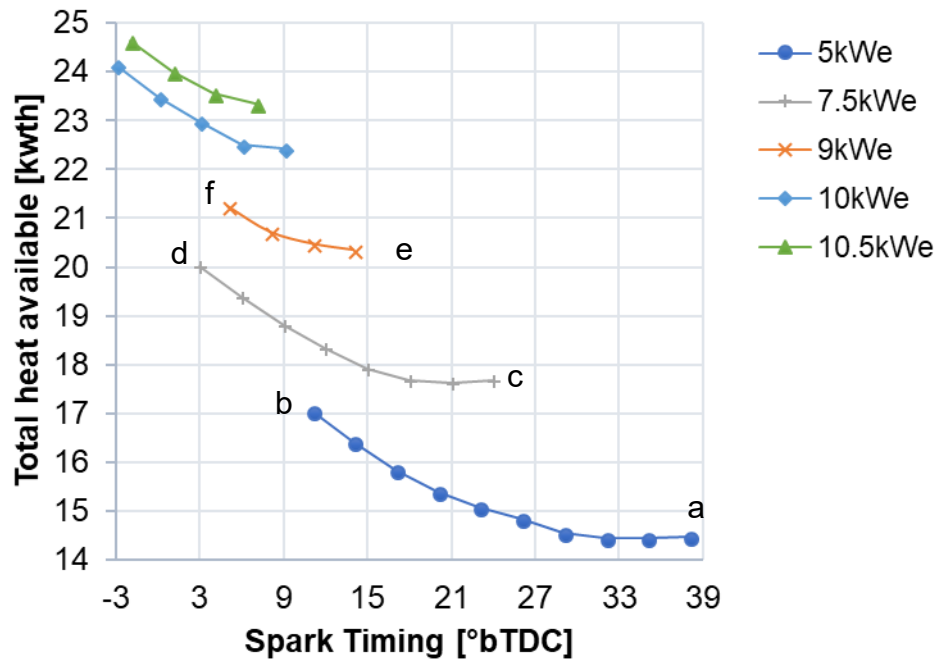


Figure 12. Total Heat Available by retarding the ST. (IP=1.5 bar)

On *Figure 12* one can also see total heat available at the most retarded points of 5 & 7.5kWe, points *b* & *d*, are near to reach the amount of heat available on the next curve; i.e. 7.5kWe curve at ST=3°bTDC (point *d*) reached 20kWth while 9kWe curve at ST=14°bTDC (point *e*) produced 20.35kWth in terms of available heat. Fuel consumption at points *d* & *e* was 9.96 and 10.63 mg/Nm³ (*Figure 13*). The same analysis can be done for 5kWe curve at ST=11°bTDC (point *b*) compared with 7.5kWe curve at ST=24°bTDC (point *c*); thermal power available was 17.05 and 17.67kWth while fuel consumption was 7.95 and 9.14 mg/Nm³ respectively for points *b* & *c*.

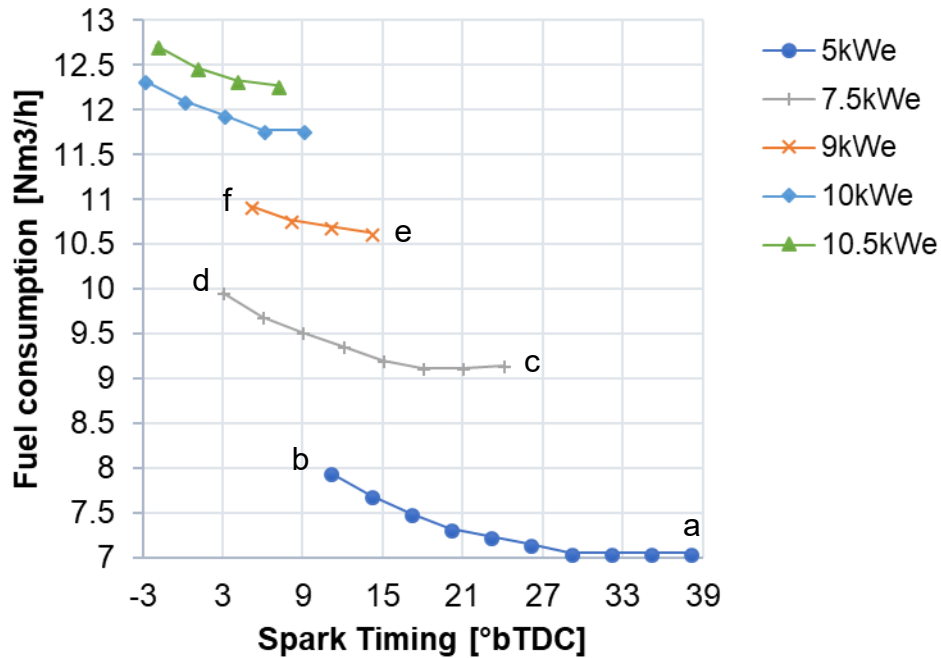


Figure 13. Fuel consumption vs spark timing. (IP=1.5 bar)

To have more complete information, *Figure 14* shows the electric efficiency of both curves, 5 and 7.5kWe. As known on internal combustion engines, the electric efficiency at low loads are always lower and hydrogen engines are not the exception. The maximum electric efficiency at 5 and 7.5kWe was 24.14% and 27.66% respectively. The amount of unburned hydrogen measured on the tests were 2.5 and 1.9% constant for 5 and 7.5kWe respectively, also shown on the same figure.

4.3.1.1. Results

The engine worked without any problem on whole the measuring range even on highly retarded spark timings, giving the possibility of producing even 17.83% higher heat available. Better fuel economy may be reachable by using retarded spark timing with lower

electric power outputs when no electric storage or selling-to-the-grid possibility is available. Nonetheless, this may be a hasty conclusion since there are no points with exactly the same thermal power available to compare. Furthermore, as shown in *Figure 14*, the amount of unburned hydrogen incremented for leaner mixtures.

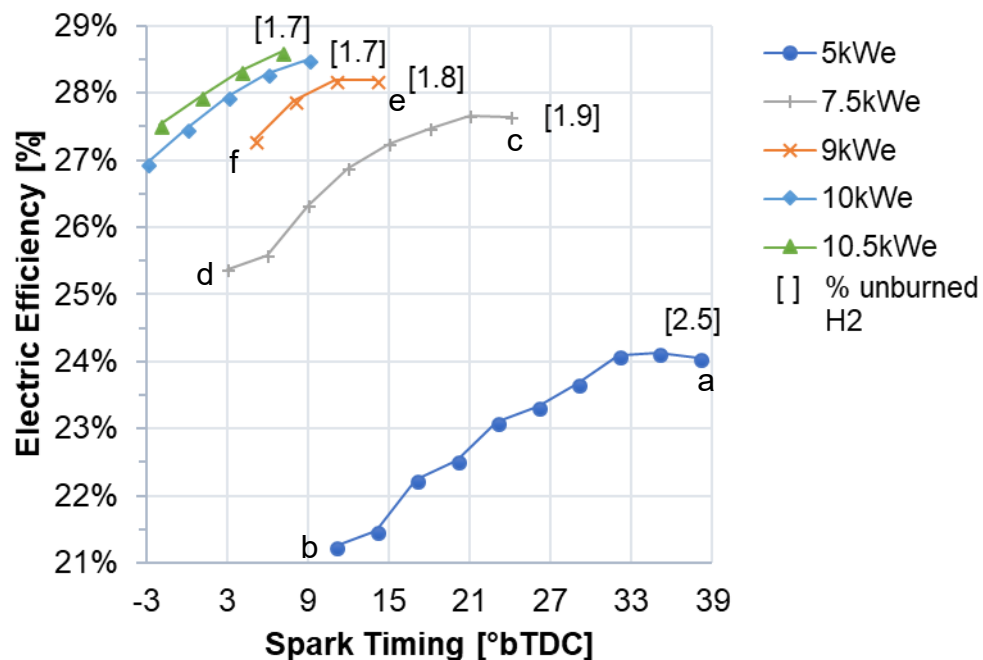


Figure 14. Electric Efficiency at part loads and higher loads. (IP=1.5 bar)

4.3.2. Higher electric power test

In order to test the possibility of reaching higher electric power output tests were done at 10 and 10.5kWe at MBT and retarding until the NO emissions reached a minimum value. Total heat available, fuel consumption and electric efficiency are also shown on *Figure 12*, *Figure 13* & *Figure 14* respectively to make contrast with part load test of the

previous section. In addition, on *Figure 15* NO emissions are shown as being the decision-making factor of this test. A superior bar is also shown over each point of the figure representing the 20% estimated percentage of NO₂ based on the data of a study of NO_x emissions on hydrogen engines run by Cornell University (Homan, de Boer, & McLean, 1983).

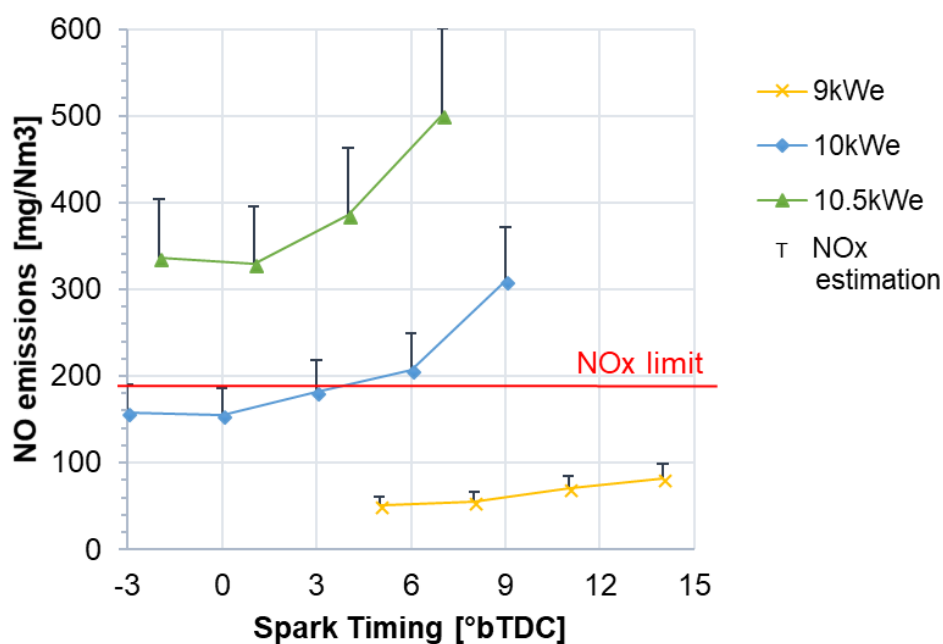


Figure 15. Emissions at higher loads. (IP=1.5 bar)

The results were not satisfactory since NO_x estimation was over or too near to the limit even when all the optimized settings were used. In fact, it's not surprise due to the richness of the mixture at 10 and 10.5kWe was $\lambda \approx 1.8$ and 1.7 respectively. Nevertheless, is worthy to compare these results with the data from the literature, where 2000 ppm NO_x are registered as usual at $\lambda = 1.7$ (Verhelst & Wallner, Hydrogen-fueled internal combustion engines, 2009), while 508 ppm NO were measured for the same mixture

richness at 10.5kWe ST=1°bTDC; this, with the 20% NO₂, gives 610 ppm NO_x emissions that is less than the third part of the 2000 value of the literature.

4.4. OPTIMIZED MAPS

Finally, two optimized ignition maps were build up as required by Van Wingen n.v.; one with MBT and the other with retarded ignition to get the lowest emissions possible without compromising the electrical efficiency. *Figure 16* shows NO emissions and NO_x estimation for both maps. *Figure 17*, in the other hand, shows the electric efficiency of both maps.

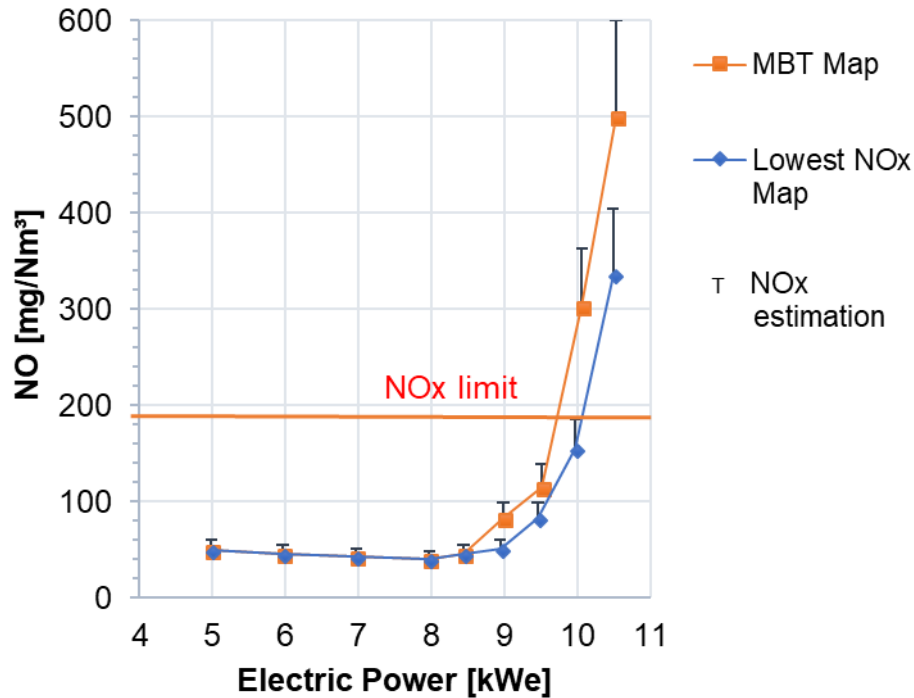


Figure 16. MBT and Minimum Retard to reduce NO_x. (IP=1.5 bar)

On the MBT map presented on *Figure 16* one can notice two important facts about the emissions of the engine on the MBT map: a linear behavior at part loads until 8kWe and an exponential grow then on. Due to the exponential grow, 9.5kWe was the maximum electric power output under the NOx limit. On the lowest NOx map, spark timing was retarded less than 10°CA to diminish the emissions without compromising the electrical efficiency. In this way, emissions similar to the linear behavior at part loads were reachable at 9kWe while the estimated emissions at 9.5kWe were reduced to 100mg/Nm³. The electric efficiency reduction at 9 and 9.5kWe was no higher than 1%.

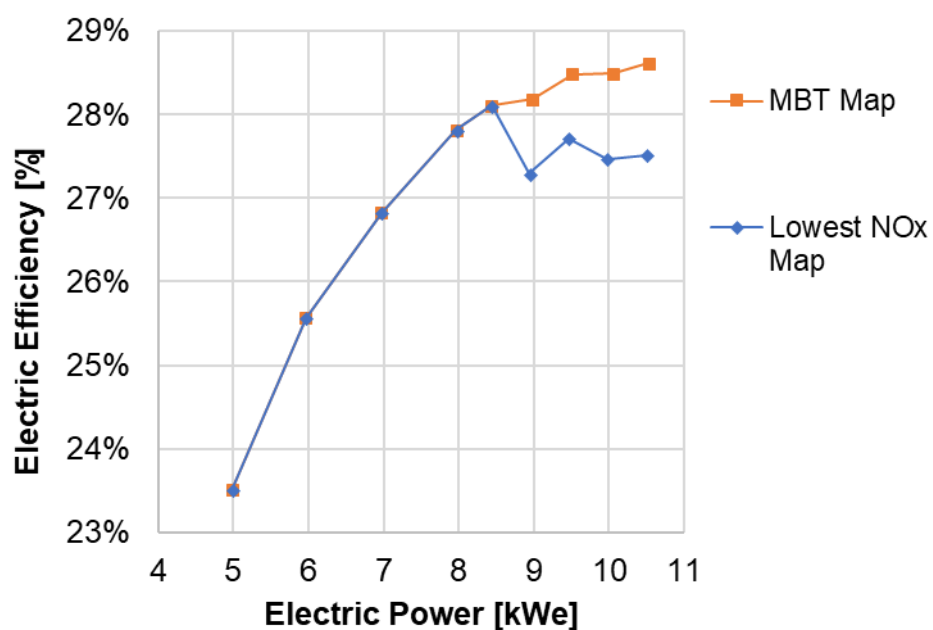


Figure 17. Electric efficiency of both mappings. (IP=1.5 bar)

4.5. POWER-TO-HEAT RATIO AND PRIMARY ENERGY SAVINGS

As stated on 2.2.1, the optimal selection of a CHP unit relies on having a primary mover capable to fulfill the pick of the electric demand of the year while having the minimum ratio between electric power of the primary mover and maximum electric demand $(P_e)_{PM}/(P_e)_{dem_max}$. In addition, the power-to-heat ratio of the CHP unit has to be the same as the power-to-heat demand ratio.

Based on this, the possibility of modifying the power-to-heat ratio without affecting the overall efficiency of the CHP can be an important improvement and a topic to be tested. On the present project tests done before on 4.2 were used to analyze this possibility; ignition timing was the only factor that showed to have an important influence over it. The results and conditions of the tests are explained in the section below.

Finally, as mentioned on 2.2, the energetic quality of a CHP unit is determined by the primary energy savings, so this factor is also studied here after.

4.5.1. Power-to-heat ratio estimation (C_{design})

In order to evaluate the power-to-heat ratio, the data of the test on 4.2.2 changing spark timing were used. For the calculations 100% of heat available on the coolant was taken into account. The heat available on the exhaust gases was used until 120°C, as a design temperature of the exhaust gases after the heat exchanger. For this case, the power-to-heat ratio shown to have a maximum value of 0.5 around 15°bTDC, while the minimum was 0.44 for retarded ignition.

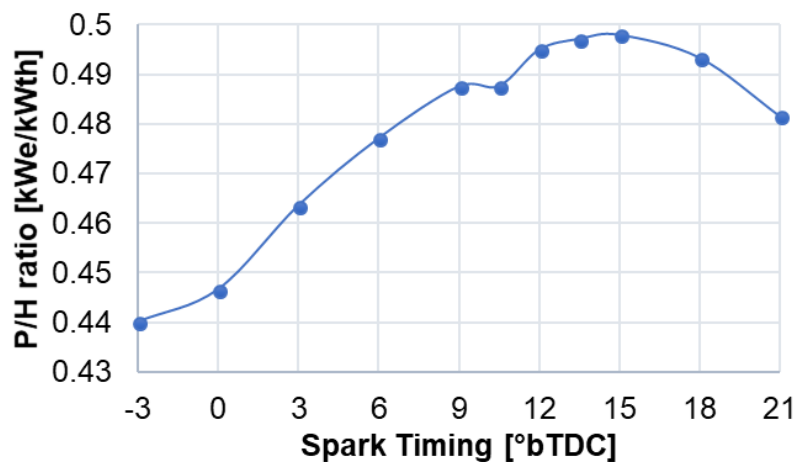


Figure 18. Power to heat ratio.

4.5.2. Primary Energy Saving Ratio

As stated on 4.2.2, 5% of heat losses from the engine block to the environment was assumed. Primary energy saving ratio was found to be over 20% even for highly retarded spark timing, cataloging the CHP as a high efficiency class according to the European Commission definition mentioned above on 2.2.

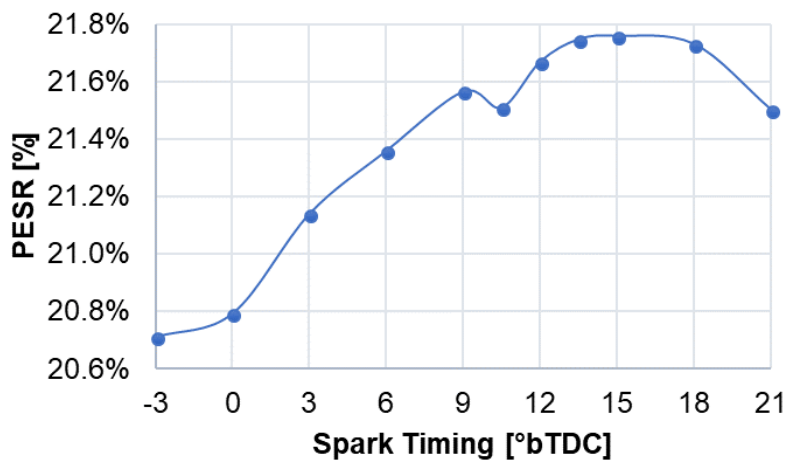


Figure 19. Primary Energy Saves Ratio.

CHAPTER V

CONCLUSIONS

5.1. CONCLUSIONS AND OPTIMIZED SETTINGS

According to the objectives of the project, the optimization of the engine in order to get the lowest emissions at 9kWe was successfully done. The explanation of the optimal choice of each engine setting as well as a comparison with the highest efficiency point is detailed hereafter. The optimal range to variate power-to-heat ratio without compromising engine performance and the primary energy savings estimation in order to guaranty a high-efficiency operation of the engine are also exposed below.

5.1.1. Start of Injection

In order to keep lower NO_x emissions, the Start of Injection must be kept less than 390°CA; NO emissions decreased from 379 to 132 mg/Nm³ by advancing the SOI from 410 to 380°CA at lambda 2. 380°CA was chosen as the optimal injection timing for the engine used in this project as it allows an air-only precooling period of the combustion chamber components before injecting the hydrogen as well as giving the flexibility of having a longer injection duration as is the case of lower injection pressure tested afterwards.

5.1.2. Spark timing

Performance curves vs. Spark Timing was divided on four sections, where zone II was defined as the optimal working range if the power-to-heat ratio is wanted to be changed due to the fact that the named zone present the highest rate of temperature rise per degree of crank angle as keeping NO emissions almost constant and far from NO_x limit. At 9kWe, zone II was defined as the zone between MBT and 10°CA retarded spark timing. In that zone, 11.5 (1.0kWth) & 7.6 (0.9kWth) percent higher heat power available was founded on the exhaust & coolant respectively, representing a 9.2% (1.9kWth) higher total heat power available. Finally, two ignition maps were established: one with the minimum advance to best torque and the other one with retarded spark timing to reduce emissions, being the second mentioned the chosen one since it gave the possibility of generating 9kWe while producing less than 100 mg/Nm³ NO_x and reaching 9.5kWe maximum power output below the NO_x limit sacrificing less than 1% of the efficiency.

5.1.3. Injection Pressure

Injection pressure was tested between 1.5 and 2.5 bar to study the influence of it over emissions. Measurements showed a decrescent trend when lowering injection pressure; 61% lower NO emissions were found at 1.5 bar compared to 2.5 bar. 1.5 bar was chosen as the optimal injection pressure for the engine tested on the present project, getting a reduction of 36% emissions at 9kW compared to the 2-bar previous injection-pressure setting of it.

5.1.4. Two ignition maps?

Part of the first objective of the project is to ensure the global efficiency of the CHP is not compromised. As the thermal efficiency relies on the design of the heat exchangers, to ensure the global efficiency of the CHP by the optimization of the ECU is indeed to ensure the electric efficiency. The optimal compromise between minimum emissions and high electrical efficiency at 9kWe was found at $SOI=380^{\circ}CA$, $ST=11^{\circ}bTDC$ and 1.5-bar injection pressure, where electric efficiency was 28.19% and NO emissions were $70.35mg/Nm^3$. That point was indeed MBT and it was used for the MBT ignition map. Nonetheless, even lower emissions were required by the sponsor, so a retarded ignition map was created in order to reach the requirements. $50.43mg/Nm^3$ NO emissions were reached by retarding spark timing to $ST=5^{\circ}bTDC$ getting 27.29% electric efficiency; less than 1% of sacrifice on electric efficiency for a reduction of 28.32% on emissions.

In contrast, maximum efficiency (28.44%) was encountered at $SOI=380^{\circ}CA$, $ST=15^{\circ}bTDC$ and 2-bar injection pressure with $158.62mg/Nm^3$ NO emissions; that is 0.25 and 1.15 percental points higher than the MBT and retarded ignition optimal settings mentioned above, but with more than twice the emissions. In that way, the optimization to get the lowest emissions possible has been demonstrated not to compromise the global efficiency of the CHP unit.

5.1.5. Power-to-heat ratio and primary energy savings

Further analysis of the data was done to evaluate the availability of varying the power-to-heat ratio. Only spark timing showed to have a significant influence over the ratio mentioned before. At 9kW, the power-to-heat ratio related with the maximum-efficiency point ($ST=15^{\circ}bTDC$) was 0.5 and it was possible to be switched down to 0.44 by retarding spark timing $18^{\circ}CA$, which represented 2.5 kWth higher total heat power available.

As the only setting that showed a significant influence over the power-to-heat ratio was spark timing, the zonal-performance analysis done for the ignition timing applies also for the power-to-heat ratio; that means Zone I has to be avoided for being consider a too-far retarded zone with a lower rise-rate of exhaust gases temperature, while Zone III and IV has to be avoided because of the increased NO emissions. In that way, reducing spark timing range to the optimal zone for best performance (Zone II), power-to-heat ratio was able to be switched from 0.49 to 0.45 that represents 1.9 kWth. An estimation of the primary energy savings for the CHP unit was done in order to verify that its energetic quality was not compromised by the variation of the power-to-heat ratio. The results were satisfactory since the primary energy savings ratio was over 20% for the complete range of ignition timing tested, which means the CHP unit can be consider as a high efficiency one even for highly retarded spark timing.

For the customer, to retard spark timing can be used as a solution to cover peaks of heat demand over the maximum thermal power produced by the CHP working with MBT. For example, when working at full load (9kW_e) and the heat demand goes over the thermal power produced by the CHP, spark timing can be retarded to reach even 1.9 kWth

more. This strategy can also reflect economic benefits since the size of the thermal storage tank, if existent, may be reduced due to the higher heat demand covered by the CHP unit. If no thermal storage tank is available, the benefit is still being the higher demand covered anyway. To enjoy the benefit, a control system may be needed in order to translate the heat demand into a signal to retard the spark timing as well as compensate the engine load.

5.2. RECOMMENDATIONS FOR FUTURE WORK

5.2.1. General recommendations

In the present project it was demonstrated the potential of retarded spark timing to produce higher heat power while reducing NO_x emissions, nonetheless, on field tests must be done with the CHP unit to validate the results.

Thermal priority and electric priority mode can be applied with part load over 50% in order to improve fuel consumption in case selling electricity to the grid is not possible.

If a condenser is to be used, care must be taken due to high water vapor fraction on the exhaust; the calculated dew point is 63°C for lambda 2.

NO_x must be measured as total next time to get more accuracy. Portable testers are recommended on the literature for being more accurate.

EGR have shown good results on the literature on reducing NO_x emissions. This can be applied to use richer mixtures, and therefore, to get higher power outputs.

5.2.2. Recommendations for the conversion of the 4.2 liters engine

As mentioned on the background, the results of this project will be used in the conversion and optimization of a 4.2L turbocharged engine in the future so, some recommendations are mentioned hereafter as a guidance.

Injection timing must be tested near top dead center (TDC) but giving an H₂-free time to the cylinder to cool down; 370-390°CA would be recommended. Nonetheless, literature review of injection timing on PFI turbocharged hydrogen engines must be also done. If NO_x emissions cannot be reduced under the limit, EGR can be used to compensate higher NO_x.

Spark timing should be tested in a wide range as done in this project, starting at MBT and retarding. Retarding the ST would drive down emissions and produce more heat, thus, turbo may gain speed; load may also need to be risen in compensation.

Pressure of injection has to be calculated in function of H₂ injection duration and intake manifold pressure; pressure over 2 bar may be needed. Correct selection of the injectors would rely on this.

The hydrogen flow meter used in this project was working at 70%FS at 9kW; Since the full scale is 18Nm³/h, a flow meter with higher capacity must be used.

REFERENCES

- Abengoa. (2007). *La necesidad de un nuevo vector energético: el hidrógeno*. Retrieved from http://www.abengoa.es/htmlsites/boletines/es/diciembre2007ext/fr_hidrogeno.htm
- Air Liquide. (2018, July 29). Gas Encyclopedia Air Liquide. Retrieved from <https://encyclopedia.airliquide.com/hydrogen>
- Alonso, J. (2017, November 1). *América Latina y el cambio climático: una carrera de fondo*. Retrieved February 28, 2018, from DW: <http://p.dw.com/p/2mpfu>
- Annex 3 of Book VI of the unified text from the secondary legislation of the Environmental Ministry (2015).
- Arbabi, P., Abbassi, A., Mansoori, Z., & Seyfi, M. (2017). Joint Numerical-Technical Analysis and Economical Evaluation of Applying Small Internal Combustion Engines in Combined Heat and Power (CHP). *Applied Thermal Engineering* (2017), 694-704. doi:10.1016/j.applthermaleng.2016.11.064
- Barbieri, E., Spina, P., & Venturini, M. (2012). Analysis of innovative micro-CHP systems to meet household energy demands. *Applied Energy* 97 (2012), 723-733. doi:10.1016/j.apenergy.2011.11.081
- Brandon, N. P., & Kurban, Z. (2017). Clean energy and the hydrogen economy. *Phil. Trans. R. Soc. A* 375: 20160400. doi:10.1098/rsta.2016.0400
- Brizuela, E., & Romano, S. D. (2003). 67.30 Combustión - 1ra Parte. Universidad de Buenos Aires - Argentina. Retrieved from <http://materias.fi.uba.ar/6730/tps.html>

- Bronkhorst. (2008, April 4). *Instruction Manual - General instructions digital Mass Flow / Pressure instruments laboratory style / IN-FLOW*. Retrieved from <https://flow.no/wp-content/uploads/sites/20/2017/08/917022-manual-general-instructions-digital-laboratory-style-and-in-flow.pdf>
- Caresana, F., Brandoni, C., Feliciotti, P., & Bartolini, C. M. (2011). Energy and economic analysis of an ICE-based variable speed-operated micro-cogenerator. *Applied Energy* 88, 659-671. doi:10.1016/j.apenergy.2010.08.016
- Cengel, Y. (2011). *Termodinámica, 7ed.* McGraw-Hill.
- Chintala, V., & Subramanian, K. (2013). A CFD (computational fluid dynamics) study for optimization of gas injector orientation for performance improvement of a dual-fuel diesel engine. *Energy* 57, 709-721.
- CIMSA. (s.f.). *Fragilización por hidrógeno*. Retrieved January 5, 2018, from http://www.cimsa.com/internet/es/cupropedia/la_corrosi_n/fragilizacion_por_hidrogeno/fragilizacion_por_hidrogeno.jsp
- Commission Decision of 19 November 2008 establishing detailed guidelines for the implementation and application of Annex II to Directive 2004/8/EC of the European Parliament and of the Council. (17.12.2008). 55-61.
- Commission Delegated Regulation (EU) 2015/2402 of 12 October 2015 reviewing harmonised efficiency reference values for separate production of electricity and heat in application of Directive 2012/27/EU of the European Parliament and of the Council. (19.12.2015). *Official Journal of the European Union*, 54-61.
- CRES & ZREU. (2001). *Training Guide on Combined Heat & Power Systems*.

de Agustín, D., Ibarra, A., Julián, I., de Sá, J., Martínez, S., & Sáez, R. (2000). Diccionario de ciencias. España: Oxford-Comlutense. Retrieved from https://books.google.be/books?id=_5-yHvJ61eQC&lpg=PP1&pg=PP1#v=onepage&q&f=false

de Santoli, L., Lo Basso, G., Albo, A., Bruschi, D., & Nastasi, B. (2015). Single cylinder internal combustion engine fuelled with H₂NG operating as micro-CHP for residential use: preliminary experimental analysis on energy performances and numerical simulations for LCOE assessment. *Energy Procedia* 81 (2015) 1077-1089.

Demuyck, J. (2013). A Fuel Independent Heat Transfer Correlation for Premixed Spark Ignition Engines. Doctoral Thesis UGent - Belgium.

Diario El Universo. (2017, July 29). *Lenín Moreno ratificó Acuerdo de París en Nuevo Rocafuerte*. Retrieved March 8, 2018, from <https://www.eluniverso.com/noticias/2017/07/30/nota/6304426/lenin-moreno-ratifica-acuerdo-paris>

Directive 2009/72/EC of the European Parliament and of the Council of 13 July 2009 concerning common rules for the internal market in electricity and repealing Directive 2003/54/EC (Text with EEA relevance). (14.8.2009). *Official Journal of the European Union*. Retrieved from <https://eur-lex.europa.eu/legal-content/EN/TXT/PDF/?uri=CELEX:32009L0072&from=EN>

Directive 2012/27/EU of the European Parliament and of the Council of 25 October 2012 on energy efficiency, amending Directives 2009/125/EC and 2010/30/EU and repealing Directives 2004/8/EC and 2006/32/EC. (14.11.2012). 1-56.

- Durán, L. (2012, August). Beneficios ambientales, sociales y tecnológicos, por la implementación de sistemas de abastecimiento energéticos, mediante el empleo de energías renovables. (sistema fotovoltaico). México D.F. Retrieved from <https://www.zaragoza.unam.mx/portal/wp-content/Portal2015/Licenciaturas/iq/tesis/beneficios%20ambientales.pdf>
- E. Van Wingen nv. (2017, February 20). *Mini-CHP*. Retrieved from https://vanwingen.be/uploads/downloads/EVW_Mini-WKK_EN_20-02-2017_LQ.pdf
- European Commission. (2011). *A Roadmap for moving to a competitive low carbon economy in 2050*. Retrieved October 25, 2017, from https://ec.europa.eu/clima/policies/strategies/2050_en
- Ferrero, D., Gamba, M., Lanzini, A., & Santarelli, M. (2016). Power-to-Gas Hydrogen: techno-economic assessment of processes towards a multi-purpose energy carrier. *Energy Procedia* 101 (2016) 50-57.
- Foro Nuclear. (n.d.). *¿Qué es y de dónde proviene el hidrógeno?* Retrieved March 14, 2018, from Rincon Educativo: <http://www.rinconeducativo.org/es/recursos-educativos/que-es-y-de-donde-proviene-el-hidrogeno>
- Frangopoulos, C. (2012). A method to determine the power to heat ratio, the cogenerated electricity and the primary energy savings of cogeneration systems after the European Directive. *Energy* 45 (2012) 52-61. doi:10.1016/j.energy.2011.12.044
- Fraunhofer Institut für Windenergie und Energiesystemtechnik (IWES). (2011). *Energiewirtschaftliche und ökologische*. Kassel - Alemania. Retrieved septiembre 13, 2017, from https://en.wikipedia.org/wiki/Power_to_gas#cite_note-1

- Fundación de la Energía de la Comunidad de Madrid [FENERCOM]. (2007). *Guía Básica de la Generación Distribuida*. Retrieved from <https://www.fenercom.com/pdf/publicaciones/guia-basica-de-la-generacion-distribuida-fenercom.pdf>
- Gahleitner, G. (2013). Hydrogen from renewable electricity: An international review of power-to-gas pilot plants for stationary applications. *International Journal of Hydrogen Energy* 38 (2013) 2039-2061. doi:10.1016/j.ijhydene.2012.12.010
- Gillingham, K. (2007, January). Hydrogen Internal Combustion Engine Vehicles: A Prudent Intermediate Step or a Step in the Wrong Direction? Stanford University, Stanford - USA. Retrieved from <http://environment.yale.edu/gillingham/hydrogenICE.pdf>
- Global Combustion Systems. (n.d.). *NOx Measurement*. Retrieved May 2018, 17, from <http://www.globalcombustion.com/nox-measurement/>
- Guervós, M. (2003, March 15). *Principales técnicas de almacenamiento de hidrógeno*. Retrieved from <http://estherguervos.galeon.com/4alm.pdf>
- Heywood, J. (1988). *Internal Combustion Engine Fundamentals*. McGraw-Hill.
- Homan, H. S., de Boer, P. C., & McLean, W. J. (1983). The effect of fuel injection on NOx emissions and undesirable combustion for hydrogen-fuelled piston engines. *International Journal of Hydrogen Energy*, 8(2), 131-146. doi:10.1016/0360-3199(83)90095-2
- Jabbar, A. I., Vaz, W. S., Khairallah, H. A., & Koylu, U. O. (2016). Multi-objective optimization of operating parameters for hydrogen-fueled spark-ignition engines. *International Journal of Hydrogen Energy*, 41(40), 18291-18299.

- Jadhao, J. S., & Thombare, D. G. (2013). Review on Exhaust Gas Heat Recovery for I.C. Engine. *International Journal of Engineering and Innovative Technology* (2), 93-100.
- Leroy-Somer. (2018). *IMfinity® 3-phase induction motors - Catalogue - Ref. 5147h_en*. Retrieved May 16, 2018, from <http://acim.nidec.com/motors/leroy-somer/downloads/catalogues>
- López, D. (2013). *Efecto de la fragilización por hidrógeno de metales sometidos a tensión*. Retrieved January 5, 2018, from <http://azterlan.blogspot.be/2013/07/efecto-de-la-fragilizacion-por.html>
- McAllister, S., Chen, J., & Fernandez-Pello, A. (2011). *Fundamentals of Combustion Processes*. New York: Springer. doi:10.1007/978-1-4419-7943-8_2
- MEGlobal. (2008). Ethylene Glycol - Product Guide. Retrieved from http://www.meglobal.biz/media/product_guides/MEGlobal_MEG.pdf
- National Association of Corrosion Engineers. (2018, January 26). *Fragilidad del hidrógeno*. Retrieved from <https://www.nace.org/Corrosion-Central/Corrosion-101/Hydrogen-Embrittlement/>
- Nemati, A., Fathi, V., Barzegar, R., & Khalilarya, S. (2013). Numerical investigation of the effect of injection timing under various equivalence ratios on energy and exergy terms in a direct injection SI hydrogen fueled engine. *International Journal of Hydrogen Energy* 38, 1189-1199.
- Olsen, D. B., Kohls, M., & Arney, G. (2010). Impact of Oxidation Catalysts on Exhaust NO₂/NO_x Ratio from Lean-Burn Natural Gas Engines. *Journal of the Air & Waste Management Association*, 60:7, 867-874. doi:10.3155/1047-3289.60.7.867

- ONU. (n.d.). *Objetivo 13: Adoptar medidas urgentes para combatir el cambio climático y sus efectos – Situación 2017*. Retrieved March 1, 2018, from <http://www.un.org/sustainabledevelopment/es/climate-change-2/>
- Pérez, J., & Merino, M. (2014). *definicion de hidrógeno*. Retrieved March 14, 2018, from definicion.de: <https://definicion.de/hidrogeno/>
- Pino, A. (2009). *Aprovechamiento de recursos energéticos renovables no integrables en la red eléctrica. el caso de la producción de hidrógeno*. Retrieved from e-REdING - Biblioteca Electrónica Universidad de Sevilla: <http://bibing.us.es/proyectos/abreproy/30127/fichero/Cap%C3%ADtulo+2+-+Producci%C3%B3n+de+Hidr%C3%B3geno.pdf>
- Policy Department A: Economic and Scientific Policy. (2010). *Decentralized Energy Systems*. European Parliament. Retrieved from <http://www.europarl.europa.eu/document/activities/cont/201106/20110629ATT22897/20110629ATT22897EN.pdf>
- Radu, R., Micheli, D., Alessandrini, S., Casula, I., & Radu, B. (2015). Modeling and Performance Analysis of an Integrated System: Variable Speed Operated Internal Combustion Engine Combined Heat and Power Unit-Photovoltaic Array. *Journal of Energy Resources Technology*, 137, 032001-1-10.
- Real Academia Española. (n.d.). *hidrógeno*. Retrieved March 14, 2018, from Diccionario de la lengua española: <http://dle.rae.es/?id=KKVuUmz>
- Registro Estatal de Emisiones y Fuentes Contaminantes [PRTR-España]. (2018, January 8). *Nox (Óxidos de Nitrógeno)*. Retrieved from <http://www.prtr-es.es/NOx-oxidos-de-nitrogeno,15595,11,2007.html>

- Ren, H., Gao, W., & Ruan, Y. (2008). Optimal sizing for residential CHP system. *Applied Thermal Engineering* 28 (2008) 514–523.
doi:10.1016/j.applthermaleng.2007.05.001
- Romero, L. (2014). *Análisis de la reducción de consumos energéticos en un edificio al integrar un sistema fotovoltaico y de micro-cogeneración mediante trnsys*. Retrieved from e-REdING: <http://bibing.us.es/proyectos/abreproy/70549/>
- Salvi, B. L., & Subramanian, K. A. (2016). Experimental investigation on effects of compression ratio and exhaust gas recirculation on backfire, performance and emission characteristics in a hydrogen fuelled spark ignition engine. *International Journal of Hydrogen Energy*, 41(13), 5842-5855.
- Scheepers, M., Bauknecht, D., Jansen, J., de Joode, J., Gómez, T., Pudjianto, D., . . . Strbac, G. (2007). *Regulatory Improvements for Effective Integration of Distributed Generation into Electricity Distribution Networks - Summary of the DG-GRID project results*. Retrieved from https://ec.europa.eu/energy/intelligent/projects/sites/iee-projects/files/projects/documents/dg-grid_summary_of_the_dg_grid_project_results.pdf
- Scheven, A. v., Steiner, L., & Völker, D. (2013). *Evaluationsbericht - vorgelegt von der Forschungsgruppe Regenerative Energien unter der Leitung von Prof. Dr. Thomas Hartkopf Technische Universität Darmstadt*. Alemania: EENERGY. Retrieved from http://www.digitale-technologien.de/DT/Redaktion/DE/Downloads/ab-elektrotechnik-bereich.pdf?__blob=publicationFile&v=2

Schlumberger. (s.f.). *fragilidad por hidrógeno*. Retrieved January 5, 2018, from Oilfield

Glossary:

http://www.glossary.oilfield.slb.com/es/Terms/h/hydrogen_embrittlement.aspx

Sharma, S. K., Goyal, P., & Tyagi, R. K. (2015). Hydrogen-Fueled Internal Combustion Engines: A Review of Technical Feasibility. *International Journal of Performability Engineering* 11(5), 491-501.

Sierens, R., & Verhelst, S. (2000). Experimental Study of a Hydrogen-Fueled Engine. *Journal of Engineering for Gas Turbines and Power* 123 (1), 211-216.
doi:10.1115/1.1339989

Sira Certification Service. (2014, May). *Technical Endorsement 4 - Example calculations associated with the measurment of gases and vapours using instrumental techniques*. Retrieved May 17, 2018, from <http://www.csagroupuk.org/wp-content/uploads/2015/05/TE4-Example-Calculations.pdf>

Subramanian, V., Mallikarjuna, J., & Ramesh, A. (2007). Effect of water injection and spark timing on the nitric oxide emission and combustion parameters of a hydrogen fuelled spark ignition engine. *International Journal of Hydrogen Energy* 32 (2007), 1159-1173.

THE World University Rankings. (2017). *Ghent University*. Retrieved from <https://www.timeshighereducation.com/world-university-rankings/ghent-university>

UGent. (n.d.). *Ghent University Academic Bibliography*. Retrieved September 19, 2017, from <https://biblio.ugent.be/person>

Vargas, C. (2011). Retrieved May 8, 2018, from *Mente ácida*: <https://menteacida.com/no2-dioxido-de-nitrogeno.html>

- Verhelst, S. (2014). Recent progress in the use of hydrogen as a fuel for internal combustion engines. *Hydrogen Energy*, 1071-1085. doi:10.1016/j.ijhydene.2013.10.102
- Verhelst, S., & Wallner, T. (2009). Hydrogen-fueled internal combustion engines. *Progress in Energy and Combustion Science* 35, 490-527. doi:10:1016/j.pecs.2009.08.001
- Verhelst, S., Wallner, T., Eichlseder, H., Naganuma, K., Gerbig, F., Boyer, B., & Tanno, S. (2012). Electricity Powering Combustion: Hydrogen Engines. *Proceedings of the IEEE* 100(2), 427-439. doi:10.1109/jproc.2011.2150190
- VLAREM II, article 5.43.2 (2018-05-04).
- Wallner, T., Scarcelli, R., Lohse-Busch, H., Wozny, B., & Miers, S. A. (2009). Safety Considerations for Hydrogen Test Cells. *3rd ICHS Conference on Hydrogen Safety*, 1-14.
- Wang, L., Yang, Z., Huang, Y., Liu, D., Duan, J., Guo, S., & Qin, Z. (2017). The effect of hydrogen injection parameters on the quality of hydrogen-air mixture formation for a PFI hydrogen internal combustion engine. *International Journal of Hydrogen Energy* 42, 23832-23845. doi:10.1016/j.ijhydene.2017.04.086
- WWF. (n.d.). *América Latina y el Caribe toman acciones frente al cambio climático*. Retrieved March 1, 2018, from <https://www.worldwildlife.org/climatico/america-latina-y-el-caribe-toman-acciones-frente-al-cambio-climatico>
- Zoulias, E., & Lymberopoulos, N. (2008). *Hydrogen-based Autonomous Power Systems - Techno-economic Analysis of the Integration of Hydrogen in Autonomous Power Systems*. Greece: Springer. doi:10.1007/978-1-84800-247-0